MATERIALS CHEMISTRY FRONTIERS

REVIEW

View Article Online
View Journal | View Issue

Cite this: *Mater. Chem. Front.*, 2025, **9**, 3245

Recent advances in boron-based room-temperature phosphorescence materials: design strategies, mechanisms, and applications

Siying Peng, Xueqi Cai, Qiuyu Zhang, Yitong Sun, Liyan Zheng, Qiue Cao and Yonggang Shi *

Received 15th July 2025,
Accepted 15th September 2025

DOI: 10.1039/d5qm00513b

rsc.li/frontiers-materials

Boron-based room-temperature phosphorescence (RTP) materials have garnered considerable attention due to their unique photophysical properties and diverse application potential. Nevertheless, systematic discussion on the design strategies, excited state control mechanisms, and practical applications of such molecules remains scarce. This review systematically analyzes the structure–property relationships in boron-based RTP materials, focusing on the influence of key structural factors such as their coordination modes, the number and position of substituents, and the design of host–guest systems. These factors enable precise control over the phosphorescence lifetime and the emission wavelength of the materials. Boron-based RTP materials demonstrate promising applications particularly in anti-counterfeiting, light-emitting displays, and biological imaging. Moreover, this review outlines future research directions and challenges, offering a theoretical foundation for the development of novel RTP materials.

1. Introduction

Room-temperature phosphorescence (RTP) materials demonstrate diverse application potential in anti-counterfeiting, light-emitting displays, and biological imaging owing to their long luminescence lifetimes and large Stokes shifts.[1–11] Conventional phosphorescent materials, which predominantly rely on noble metal complexes, exhibit excellent luminescent properties. However, their high cost and environmental toxicity hinder large-scale applications.[12] Consequently, the design and synthesis of high-performance, eco-stable, and environmentally benign pure organic RTP materials have become a prominent research priority in contemporary materials science.[13,14]

In purely organic systems, achieving RTP emission remains a major challenge due to the inherently weak spin–orbit coupling (SOC), spin constraints during the $S_1 \rightarrow T_1$ transition, and the substantial energy gap between singlet and triplet states (ΔE_{ST}).[15–18] These factors collectively cause inefficient intersystem crossing (ISC).[19] To overcome these limitations, researchers have developed strategies to enhance SOC and modulate the ISC process,[11,20–23] including (i) the introduction of heavy atoms[24–26] (*e.g.*, Br and I) and heteroatoms[27,28] (*e.g.*, O, S, and B) and (ii) implementation of crystal engineering,[29] polymerization,[22,30–32] and host–guest doping systems.[33–37] These approaches effectively suppress non-radiative decay pathways of triplet excitons, thereby enhancing phosphorescence performance.

The empty p-orbital in boron-based compounds interacts with π-systems to enhance SOC and improve ISC efficiency, thereby generating abundant triplet excitons. Boron-based RTP materials can be broadly categorized into two structural classes: three-coordinate (sp^2) and four-coordinate (sp^3) boron complexes.[38,39] In three-coordinate boron systems, the empty p-orbital acts as a strong electron acceptor that conjugates with electron donors to form donor–acceptor (D–A) structures.[40,41] This structural arrangement promotes efficient intramolecular charge transfer (ICT) and markedly improves ISC efficiency. Four-coordinate boron compounds effectively suppress vibrational/rotational motions, thereby stabilizing triplet excitons.[38,42,43] Both structural motifs impart excellent RTP properties while enabling precise control over emission color, lifetime, and environmental responsiveness *via* molecular design, host–guest interactions, and polymeric rigid environments (Fig. 1). Despite substantial progress in developing three- and four-coordinate boron-based RTP materials, current research lacks comprehensive reviews that systematically examine their molecular design strategies, excited-state regulation mechanisms, and practical applications.

This review examines advances in the molecular design and performance optimization of boron-containing organic RTP materials. We first analyze how boron coordination modes regulate excited states, electronic structures, and molecular rigidity and comprehensively evaluate the impact of different boron coordination structures on RTP performance. This review further

School of Chemical Science and Technology, National Demonstration Center for Experimental Chemistry and Chemical Engineering Education, Yunnan University, Kunming, Yunnan 650091, P. R. China. E-mail: yonggangshi@ynu.edu.cn

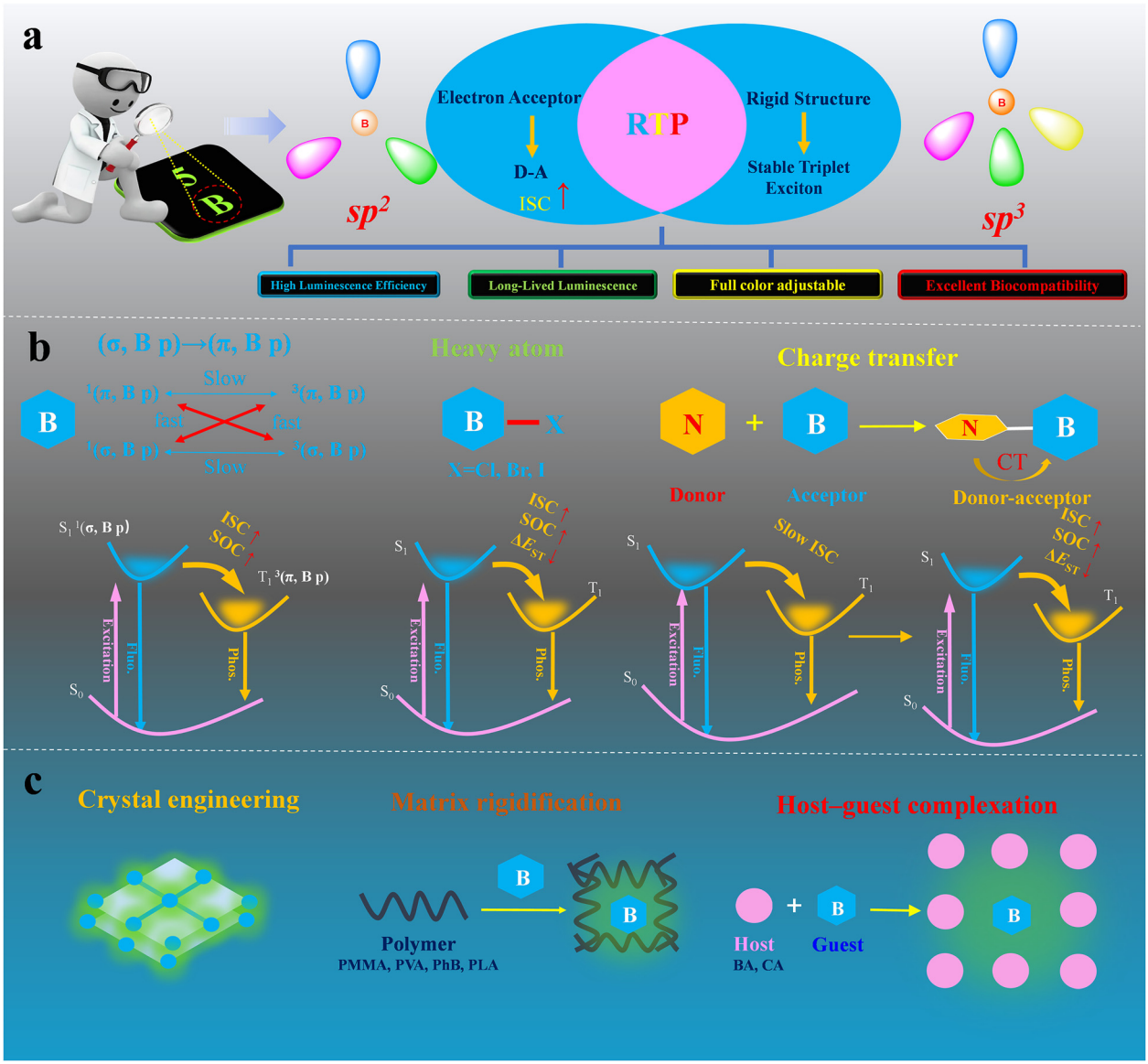

Fig. 1 (a) Boron-based room temperature phosphorescent materials; (b) strategies of molecular design, including the (σ, B p) → (π, B p) transition mechanism in three-coordinate boron systems, heavy atom introduction, and donor–acceptor system design to facilitate ISC and stabilize triplet states; (c) strategies for room-temperature phosphorescence efficiency enhancement, such as crystal engineering, host–guest doping, and suppression of non-radiative decay *via* rigidification.

compares three-coordinate and four-coordinate boron systems in terms of luminescence efficiency, lifetime, phosphorescence mechanisms, and practical applications.

2. Boron-based RTP materials

This study systematically elaborates on two categories of boron-based RTP materials: three-coordinate and four-coordinate systems. In the three-coordinate system, we initiated with simple boric acid and progressively expanded to phenylboronic acid and triarylborane systems, effectively regulating phosphorescence performance through the introduction of charge transfer (CT) effects. The four-coordinate system is based on the difluoroboron-β-diketonate framework, where structural modifications were implemented through a dual strategy: on the one hand, various substituents were introduced at both sides of the framework. On the other hand, the coordinating oxygen atoms were replaced with nitrogen, sulfur, or carbon atoms possessing lower electronegativity, thereby constructing four-coordinate boron-based phosphorescence materials with rich structural diversity. These molecular design strategies not only expand the structural diversity of boron-based phosphorescent materials but also provide crucial pathways for achieving highly efficient and long-lived RTP.

2.1 Three-coordinate boron RTP materials

In three-coordinate boron RTP materials, the boron (B) atoms typically adopt sp^2 hybridization, forming σ bonds with three

substituents while maintaining an empty p_z orbital. This electron-deficient characteristic makes three-coordinate boron atoms strong electron acceptors. The empty p_z orbital effectively stabilizes the lowest unoccupied molecular orbital (LUMO) of the boron-based compounds, enhancing their electron affinity and facilitating electron transfer between the boron center and surrounding substituents. This section will explore the influence of different substituents on the performance of three-coordinate boron RTP materials.

2.1.1 Boric acid. Boric acid (BA), a metal-free and carbon-free boron-based compound, is structurally characterized by the hydroxyl substitution of three hydrogen atoms in borane. This distinctive structural modification endows it with remarkable advantages in room-temperature phosphorescence (RTP) performance, including the extended phosphorescence lifetime and enhanced quantum yield.[44] Regarding the luminescence mechanism of BA's RTP, three primary viewpoints prevail in academia: first, the cluster-triggered emission (CTE) mechanism achieved through weak through-space conjugation of oxygen n-electrons;[45] second, the discovery that B–O–O–B impurities present in commercial BA samples undergo O–O bond cleavage under photoexcitation to form B–O free radicals, thereby generating RTP with a lifetime of approximately 1 s;[46,47] third, the confirmation that thermally induced defects can initiate millisecond-scale phosphorescence.[47] Notably, while pure BA itself lacks intrinsic phosphorescent properties,[48] its unique rigid structure and dense hydrogen-bonding network make it an ideal host material for constructing highly efficient doped RTP fluorescent systems (Fig. 2).

BA functions as an efficient host material in RTP doping systems, demonstrating several distinctive advantages. Firstly, its pyrolysis product, boron trioxide (B_2O_3), forms a rigid environment that effectively suppresses non-radiative quenching of triplet excitons. Secondly, the highly cross-linked structure of B_2O_3, composed of triangular BO_3 units connected by oxygen bridges, provides anchoring sites for fluorescent dopants, further inhibiting non-radiative transitions and enhancing RTP performance.[49–51] These favorable properties have prompted extensive research on BA-doped RTP materials. For instance, Tang *et al.* developed a highly efficient system by embedding levofloxacin (Lev) in a BA matrix. The resulting complex exhibited exceptional luminescence properties with a photoluminescence quantum yield of 63.8% and a lifetime of 0.74 s, representing an approximately 50% quantum yield enhancement compared to undoped Lev. This performance improvement can be attributed to three key factors: (i) the BA matrix's confinement effect stabilizing triplet excitons, (ii) B–C bond formation activating radiative decay, and (iii) oxygen isolation preventing environmental quenching.[52]

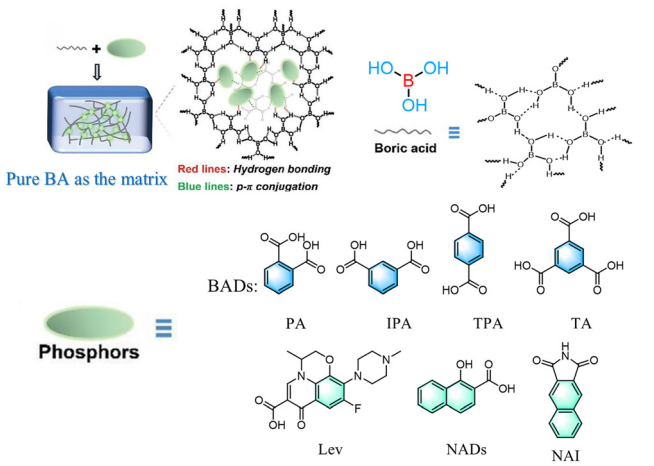

Fig. 2 Host (BA)–guest (Lev/BADs/NADs/NAI) system proposed mechanism for RTP material formation. Reproduced with permission from ref. 55. Copyright 2024 Advanced Functional Materials.

Our research group employed a similar strategy to incorporate benzoic acid derivatives (BADs) into a BA matrix, successfully preparing a series of BA-based composites (BADs@BA). These composites exhibited significantly enhanced phosphorescence quantum yield (Φ_P) compared to the host material. Notably, IPA@BA demonstrated a Φ_P of 38.23%, while TPA@BA achieved 68.73% with an exceptionally long phosphorescence lifetime.[53] Subsequently, we expanded this system by embedding naphthoic acid derivatives (NADs) into the BA matrix, synthesizing NADs@BA composites. Among these, 1-hydroxy-2-naphthoic acid (1H2NA)@BA exhibited remarkable performance with a lifetime reaching 1.7 s and demonstrated low-concentration doping luminescence capability.[54]

Lin *et al.* employed BA as a host matrix to develop NAI/BO composites through host–guest doping with 2,3-naphthalimide (NAI). The resulting material exhibited exceptional RTP properties, achieving organic long-persistent luminescence (OLPL) persistence for up to 180 minutes. Notably, by modifying the guest molecules, the researchers successfully tuned the OLPL emission color from green to orange-red, demonstrating the system's remarkable versatility in optical modulation.[56] It is important to clarify that long persistent luminescence (LPL) is a phenomenon in which light energy is pre-stored and slowly released through long-term afterglow emission. Although the light generation mechanism differs from that of conventional RTP, the emission still originates from the radiative transition of triplet excitons. Therefore, in this study, it is still categorized within the realm of phosphorescence emission.[57]

These superior material properties originate from the BA matrix's unique network structure, which effectively disperses and immobilizes luminescent molecules through single-molecule confinement. This spatial confinement effect creates an ideal platform for achieving highly efficient single-molecule RTP.

2.1.2 Phenylboronic acids, phenylboronic esters, and their derivatives. Pure boric acid ($B(OH)_3$) exhibits no intrinsic RTP properties and is rarely utilized as a standalone luminescent material. However, strategic structural modifications can confer RTP activity. Specifically, replacing one hydroxyl group with a benzene ring or its derivatives introduces two key features: (i) a pronounced charge transfer effect and (ii) p–π conjugation between the aromatic π-electrons and boron's empty p-orbital. These modifications optimize the singlet–triplet energy level arrangement and improve ISC efficiency. Therefore, it is possible

Table 1 Photophysical properties of phenylboronic acids, phenylboronic esters, and their derivatives

Sample	Environment	λ_F [nm]	τ_F [ns]	λ_P [nm]	τ_P [ms]	Φ_P [%]	PLQY [%]	Ref.
1	Crystal	322[a]	4.9 × 10^8 [b]	482	1200	—	18	58
2	Crystal	329[a]	3.5 × 10^8 [b]	494	950	—	66	58
2	5 wt% in CA	—	—	406	5080	16.1	—	61
3	Crystal	370[a]	9.2 × 10^8 [b]	488	1700	—	53	58
4	Crystal	339[a]	1.2 × 10^8 [b]	498	250	—	10	58
5	Crystal	331[a]	—	501	180	—	7.3	58
6	Crystal	558[a]	—	558	16	—	0.92	58
7	Crystal	331[a]	5.510^8 [b]	503	1600	—	77	58
8	Crystal	—	—	483	713	—	—	59
9	Crystal	—	—	488	2240	—	—	59
10	Crystal	—	—	506	1110	—	—	59
11	Crystal	—	—	493	129	—	—	59
12	Crystal	—	—	492	1280	—	—	59
13	In PVA	368	—	428	730	—	—	60
14	In PVA	360	—	468	2240	11.2	—	60
15	In PVA	334	—	476	220	—	—	60
16	0.167 wt% in PVA1977	369	8.7	520	900	10.67	—	62
17	In PVA1977	—	—	—	—	—	—	62
18	In PVA1977	—	—	—	—	—	—	62
19	1 mol% in γ-CD	340	—	440	310	—	6.1	63
20	0.3 mol% in γ-CD	372	—	470	4650	32.8[c]	38.6[c]	63
21	1 mol% in γ-CD	357	—	510	220	—	4.7	63
22	1 mol% in γ-CD	336	—	535	720	—	22.2	63
23	1 mol% in γ-CD	396	—	605	140	—	46.2	63
24	Crystal-YG	335	8.07	511	0.011	0.48	—	64
24	Crystal-C	335	7.62	463	0.009	0.95	—	64
24	Crystal-B	335	7.80	434	0.005	0.62	—	64
25	In THF	374	6.65	—		—	0.26	67
25	Crystal	366	8.65	553	0.21	—	0.33	67
26	In THF	364	7.88	—		—	0.43	67
26	Crystal	367	8.91	550	7.2	—	0.37	67
27	In THF	348	6.74	—		—	0.47	67
27	Crystal	368	9.69	553	264	—	0.42	67
28	In THF	363	8.75	—	—	—	0.39	67
28	Crystal	370	8.44	545	430	—	0.38	67
29	In THF	363	6.81	—	—	—	0.22	67
29	Crystal	366	8.11	525	0.01	—	0.44	67
30	Crystal (*n*-30)	490, 520	—	530	61	—	3.0	68
30	Crystal (c-30)	420, 450, 490, 520	—	525	15	—	1.0	68
31	Crystal	520	—	—	—	—	0.6	68

[a] Delayed fluorescence emission wavelength. [b] Average delayed fluorescence lifetime. [c] The Φ_P and PLQY with photo-activation. Abbreviations: PVA: polyvinyl alcohol, CA: cyanuric acid, and γ-CD: γ-cyclodextrin.

to develop RTP materials from phenylboronic acid and its ester derivatives. Table 1 shows the key photophysical parameters of the compounds in order of discussion: maximum wavelengths of fluorescence (λ_F) and phosphorescence (λ_P), lifetimes (τ_F and τ_P), and both phosphorescence and photoluminescence quantum yields (Φ_P and PLQY).

Yuasa *et al.* made significant breakthroughs in crystallographic studies of phenylboronic acid **1** (Fig. 3) and its derivatives (**2–7**), demonstrating their remarkable RTP properties. Their research revealed that crystal **1** exhibits distinct blue phosphorescence (482 nm) at room temperature with an extended lifetime of 1.2 s.[58] Building upon these findings, Li *et al.* employed an electron-donating substitution strategy to further optimize the system's performance. By introducing methoxy groups at the *para* position, they synthesized (4-methoxyphenyl)boronic acid (**9**) and its derivatives (**8** and **10–12**), whose crystals demonstrated exceptional phosphorescence properties, including (i) a remarkable lifetime of 2.24 s (among the highest reported for single-component organic small

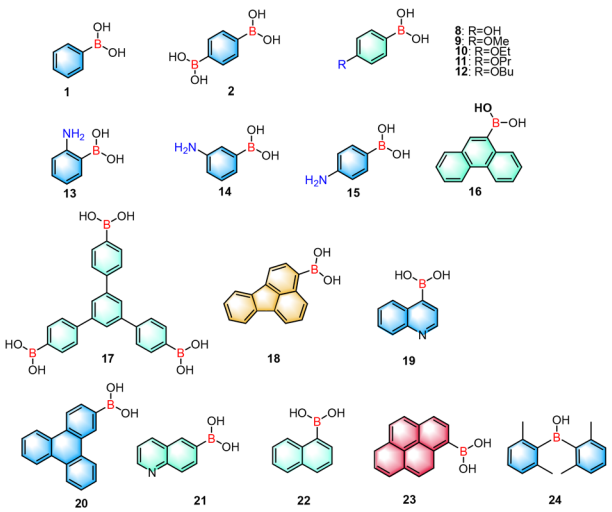

Fig. 3 Phenylboronic acid and its derivatives (compounds **1**, **2**, and **8–24**).

molecules at that time) and (ii) blue-green phosphorescence emission.[59] Nevertheless, these materials still face key challenges, particularly the limited phosphorescent color tunability and the difficulty in simultaneously enhancing both quantum yield and lifetime. To address these limitations, Yu *et al.* developed an innovative approach by doping amino-substituted phenylboronic acid (**13–15**) into a hydroxyl-rich polyvinyl alcohol (PVA) matrix. Their study revealed that the multiple hydrogen-bond network formed between *meta*-substituted 3-aminophenylboronic acid (**14**) and PVA effectively suppresses non-radiative transitions of triplet excitons, achieving a remarkable phosphorescence lifetime of 2.24 s and a Φ_P of 11.2%. Furthermore, through Förster resonance energy transfer (FRET) mechanisms and co-doping with fluorescent dyes, they successfully tuned the RTP emission from green to orange, overcoming the color limitation of conventional RTP materials.[60] Chen *et al.* advanced this host–guest doping strategy by constructing a novel hydrogen-bond network using 1,4-benzene-diboronic acid (**2**) and cyanuric acid (CA). This system established a record phosphorescence lifetime of 5.08 s for organic small molecules at that time. By precisely controlling the hydrogen-bond network density, they significantly enhanced the Φ_P from 16.1% to 37.6%, demonstrating simultaneous optimization of both phosphorescence efficiency and lifetime.[61] These studies not only elucidate the crucial role of hydrogen-bond networks in stabilizing triplet excitons but also establish effective design strategies for high-performance, color-tunable organic RTP materials.

In recent years, polycyclic aromatic hydrocarbon (PAH) systems have garnered significant attention in RTP research due to their unique electronic structures and luminescence properties. Compared to benzene derivatives, PAH's rigid frameworks and extended π-conjugated systems more effectively suppress non-radiative transitions, substantially enhancing phosphorescence performance. Chen *et al.* demonstrated that 9-phenanthrenylboronic acid (**16**) and its derivatives (**17** and **18**) doped in PVA matrices exhibit excellent phosphorescence under 405 nm excitation, achieving Φ_P = 10.67% with τ_P = 0.9 s.[62] Ma *et al.* advanced this field through molecular design, synthesizing various polycyclic BA derivatives (**19–23**). Notably, 2-triphenylenylboronic acid demonstrates excellent performance through host–guest interactions and hydrogen-bond networks, simultaneously realizing an ultra-long τ_P = 4.65 s and a high Φ_P = 32.8% under ambient conditions, and surpassing most reported organic RTP materials.[63] These studies establish crucial design principles for developing high-efficiency, long-lifetime phosphorescent materials.

In the study of diarylboronic acid systems, Pan *et al.* successfully prepared three crystalline polymorphs (crystal-YG, crystal-C, and crystal-B) by introducing two aromatic rings onto the boron atom (**24**). Through systematic investigation of the structural characteristics of these different polymorphs, they discovered that all these materials could achieve microsecond-scale RTP emission.[64] These studies have established important design principles for developing high-efficiency, long-lifetime phosphorescent materials.

Phenylboronic acid derivative-based RTP materials have attracted considerable interest in optoelectronics due to their tunable photophysical properties. However, significant changes in phosphorescence characteristics occur when the BA hydroxyl groups ($-B(OH)_2$) are substituted with alkoxy groups to form borate esters ($-B(OR)_2$), a phenomenon that has attracted widespread research attention.

Fukushima *et al.* first reported excellent RTP properties in phenylboronate compounds.[65] However, subsequent research by Hudson *et al.* revealed that the observed RTP phenomenon was actually induced by trace impurities rather than being an intrinsic property of phenylboronates themselves. After rigorous purification, the RTP characteristics of phenylboronates completely disappeared, while controlled doping could reproduce long-lived afterglow.[66] This finding emphasizes the importance of material purification in photophysical research. This contrast primarily stems from altered intermolecular interactions: the hydroxyl groups in phenylboronic acids form extensive hydrogen-bond networks that effectively stabilize triplet excitons and suppress non-radiative transitions, thereby enhancing phosphorescence. In contrast, alkoxy substitution in phenylboronic esters disrupts these hydrogen-bond networks, markedly reducing triplet exciton stabilization. Despite these challenges, recent advances show that strategic molecular design and host–guest doping approaches can enable efficient RTP emission in borate ester systems.

In 2017, Yuasa *et al.* made significant breakthroughs in the study of phenylboronic acid derivatives. By employing cyclic boronic esterification methods and introducing halogen atoms (F, Cl, Br, and I) at the *para*-position of the molecules, they successfully prepared materials exhibiting long-lived room-temperature phosphorescence (RTP). The study revealed that as the atomic number of halogens increased, the phosphorescence lifetime gradually decreased, validating that the heavy atom effect can effectively promote the intersystem crossing process. Particularly noteworthy was their development of diboronic ester compound **7** (Fig. 4), which demonstrated an extended phosphorescence lifetime of 1.6 s.[58] Subsequently, Yang *et al.* further expanded this system. Using 4-(carbazol-9-yl)phenylboronic acid as the foundation, they prepared a series of novel derivatives through cyclic esterification reactions with various diols (**25–29**). Among these, compounds **28** and **29** showed particularly

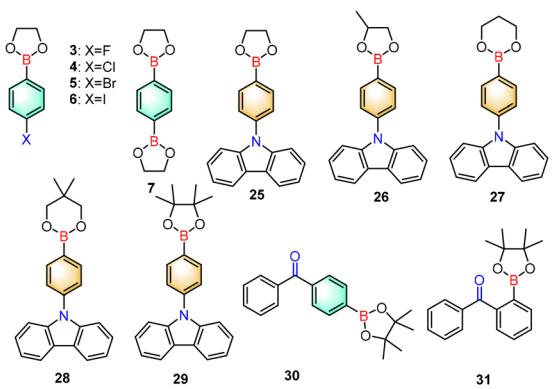

Fig. 4 Phenylboronic esters and their derivatives (compounds **3–7** and **25–31**).

outstanding performance, achieving phosphorescence lifetimes of 264 ms and 430 ms, respectively.[67] This research demonstrated that even without relying on traditional hydrogen-bonding networks, efficient triplet exciton stabilization can still be achieved through rational cyclic boronic esterification design and electron-donating group modifications.

Building upon cyclic boron esterification strategies, Yu *et al.* achieved a breakthrough in molecular design by precisely controlling the lone pair electron configuration and empty orbital arrangement of boron to regulate RTP performance. Their study revealed that *para*-substituted **30** exhibited strong RTP emission (τ_P = 61 ms) resulting from the spatial separation of lone pair of electrons and empty orbitals. In contrast, *ortho*-substituted **31** showed phosphorescence quenching due to orbital coupling. Furthermore, through controlled rotation of the borate ester groups, the team successfully achieved both polycrystalline dependent RTP modulation and temperature-responsive luminescence.[68]

Early studies generally considered simple BA structures unsuitable as ideal phosphorescent hosts due to their lack of effective luminescent groups and stable triplet energy levels. However, subsequent research demonstrated that aromatic-substituted phenylboronic acids, their esters, and derivatives exhibit remarkable RTP properties. These materials enhance ISC efficiency through synergistic effects between aromatic π-conjugation and boron's empty p-orbitals, while simultaneously stabilizing triplet excitons *via* intermolecular interactions. In-depth research studies have revealed that precise structural modifications and hydrogen-bond network optimization enable accurate control of phosphorescence performance. These systematic studies not only elucidate the unique phosphorescence mechanisms in phenylboronic acid systems, challenging conventional understanding of pure organic phosphorescent materials, but also establish crucial design principles and theoretical foundations for developing novel RTP materials.

2.1.3 Triarylboranes and their derivatives. Based on the excellent properties of phenylboronic acids and their ester derivatives, researchers have expanded research studies to triarylboranes and related compounds with unique electronic structures. Studies demonstrate that triarylboranes exhibit pronounced CT effects through the introduction of three phenyl groups, which effectively modulate the ΔE_{ST} and induce RTP characteristics. Table 2 shows the key photophysical parameters of the compounds in order of discussion: maximum wavelengths of fluorescence (λ_F) and phosphorescence (λ_P), lifetimes (τ_F and τ_P), and both phosphorescence and photoluminescence quantum yields (Φ_P and PLQY).

In 2020, Marder *et al.* reported triarylborane compounds (**32–35**), among which compounds **32** and **34** without lone electron of pairs exhibit sustained green RTP with τ = 480–680 ms. This

Table 2 Photophysical properties of triarylboranes and their derivatives

Sample	Environment	λ_F [nm]	τ_F [ns]	λ_P [nm]	τ_P [ms]	Φ_P [%]	PLQY [%]	Ref.
32	Crystal	369	—	524	680	0.3	—	69
33	Crystal	369	—	—	—	—	—	69
34	Crystal	371, 390		540, 575	480	1.2	—	69
35	Crystal	381	—	—	—	—	—	69
36	0.1 wt% in PMMA	525	12.5	610	420	—	28	70
36	10 wt% in PMMA	—	—	—	760	—	11	70
37	0.1 wt% in PMMA	445, 470	8.5	530	930	—	44	70
37	10 wt% in PMMA	—	—	—	3190	—	36	70
38	Crystal	—	3.2	446, 477 517, 562	234	1.3	1.5	71
39	Crystal	374	6.0	506, 539	64	3.1	3.8	71
40	Crystal	386	2.9	547	378	2.0	4.4	71
41	Crystal	—	—	513	—	45.0	—	72
41	Ground powder	—	—	518	—	36.0	—	72
41	Drop-cast film	—	—	545	—	22.0	—	72
42	0.5 wt% in PMMA	438	5.81	478	180	6.83	—	73
43	0.5 wt% in PMMA	439	7.07	475	110	8.88	—	73
44	0.5 wt% in PMMA	420	3.64	472	730	8.99	—	73
45	0.5 wt% in PMMA	427	4.07	521	1120	5.45	—	73
46	0.5 wt% in PMMA	429	4.57	510	1400	7.94	—	73
47	0.5 wt% in PMMA	510	16.19	—	—	—	—	74
47	Powder	490	17.8	—	—	—	—	74
48	0.5 wt% in PMMA	455[a]	5.70	550	410	9.54	—	74
48	Powder	455	7.66	—	—	—	—	74
48	1.0 wt% in PMMA	450	5.3	580	168	—	76.7	75
49	1.0 wt% in PMMA	—	—	550	129	—	88.5	75
50	Crystal	495	5.7	535[b]	232[b]	—	—	76
51	Crystal	430	7.1	276	96	—	16.3	77
52	Crystal	455	3.26	466/539	125/136	—	5.9	77
53	Crystal	423	1.03	—	—	—	—	77
54	Solid[c]	515	4.03	539	154.66	—	5.1	78
54	Solid[d]	508	5.05	504/529	176.3/185.6	—	31	78

[a] Delayed fluorescence wavelengths. [b] Open-chain radical structure of MIBNM. [c] 54 exposed to HCl. [d] 54 exposed to HCl followed by NH_3. Abbreviation: PMMA: poly(methyl methacrylate).

discovery challenged conventional design principles for organic RTP materials, which typically rely on (n, π*) transitions of lone pair electrons (*e.g.*, N and O) to facilitate ISC. Their study revealed that triarylboranes promote ISC through unique (σ,B p) → (π,B p) transitions to achieve RTP.[69] Building on this work, Wagner *et al.* developed derivatives based on the 9,10-dimesityl-dihydro-9,10-diboraanthracene (DBA) framework doped in PMMA matrices. The **37** (Fig. 5) derivative showed exceptional afterglow (τ_P = 3.2 s), while **36** exhibited persistent red phosphorescence. This binary boron system creates a strong electron-accepting center that (i) significantly lowers LUMO energy levels, (ii) enhances electron affinity, and (iii) strengthens SOC to promote efficient ISC.[70] Despite these advances, triarylborane systems typically show low Φ_P. Marder *et al.* found that direct bromination of the triarylborane skeleton (**38–40**)[71] yielded minimal RTP improvement, indicating that the heavy-atom effect alone is insufficient. Subsequently, Zhao *et al.* combined bromination with a twisted biphenyl skeleton and B–N CT effects (**41**) to suppress non-radiative transitions, achieving Φ_P = 36% in powder form, though color tunability remains limited.[72]

Based on the previously discussed B–N CT effects, our group successfully synthesized a series of aminoborane (BN) derivatives **42–46** (Fig. 6) through *para*-position dimethyl amino group incorporation into triarylboranes. In these systems, the triarylborane moiety functioned as an electron acceptor, while various push–pull substituents enabled precise control over the materials' optoelectronic properties. These materials demonstrated high Φ_P (reaching 17.34% for the **42**@PMMA film) in a nitrogen atmosphere, multicolor tunability, and excellent water resistance through photoactivation mechanisms.[73] We subsequently developed BN-based positional isomers (**47** and **48**), where the isomeric configuration of the BN group effectively modulated both ICT intensity and the ΔE_{ST}, thereby achieving precise luminescence color regulation.[74]

Similarly, Chandrasekhar *et al.* developed regioisomers (**48** and **49**) by strategically positioning triarylborane acceptors and dimethylamino donors at distinct sites on the naphthalene skeleton. These compounds exhibit dual-mode delayed fluorescence and RTP emission. Notably, compound **48** in the 1 wt% PMMA film shows reversible pH-responsive single-molecule

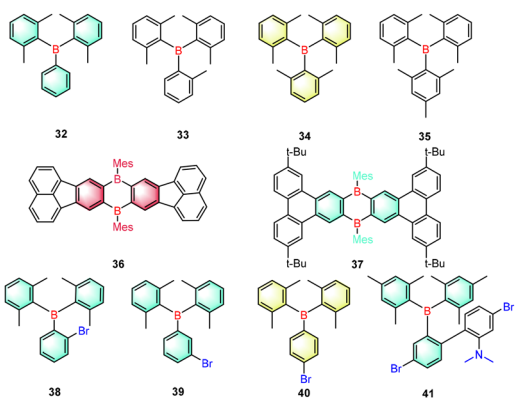

Fig. 5 Triarylboranes and their derivatives (I) (compounds **32–41**).

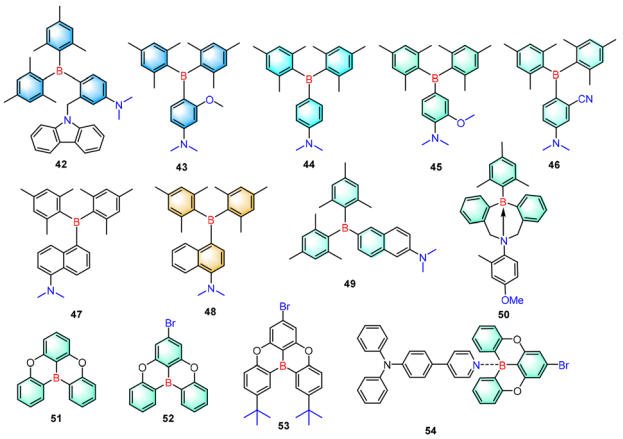

Fig. 6 Triarylboranes and their derivatives (II) (compounds **42–54**).

phosphorescence, with emission wavelengths switching between orange (580 nm) and green (550 nm).[75] This stimuli-responsive behavior, achieved through precise control of molecular conformation and intermolecular interactions, highlights its potential for advanced anti-counterfeiting applications.

The dynamic reversible B/N Lewis acid–base pair system exhibits unique phosphorescence "on–off" switching behavior, as demonstrated by Chen *et al.* in their innovative M1BNM (**50**) system. Crystal **50** initially displays only short-lived fluorescence, but ultraviolet irradiation induces reversible cleavage of the B–N coordination bond, generating an open-chain radical structure that significantly enhances ISC efficiency and activates RTP emission.[76] Li *et al.* designed a planar oxy-bridged triarylboron compound (**51–53**) and introduced a bromine atom as a heavy atom to enhance the SOC effect, significantly improving its room-temperature phosphorescence performance.[77] On this basis, they further utilized the molecule as a Lewis acid and combined it with the pyridine-containing Lewis base *N*,*N*-diphenyl-4-(pyridin-4-yl)aniline (TPAPy) through dynamic B–N coordination bonds (**54**), successfully achieving reversible control over the room temperature phosphorescence behavior: the formation of the B–N bond "turns off" the phosphorescence, while its dissociation under acid stimulation "releases" the original luminescent molecule, restoring phosphorescence emission.[78] These studies successfully extend the application of dynamic covalent chemistry to phosphorescent materials.

These remarkable properties originate from the triarylborane structure where the boron is surrounded by three aromatic rings, forming a highly delocalized π-conjugated system. This unique configuration significantly enhances the ICT effect while improving stability through interactions between boron's empty p-orbital and the aromatic π-system. Researchers have successfully developed high-performance RTP materials through strategic molecular design approaches including precise aromatic ring substituent modulation, variation of boron's numbers, introduction of polycyclic aromatic systems, and formation of D–A structures.

Three-coordinate boron RTP materials have garnered significant attention in the RTP field owing to their distinctive electronic structures and tunable optical properties. As prototypical

electron acceptors, three-coordinate boron atoms (*e.g.*, triarylboranes) interact with π-conjugated systems through their empty p-orbitals, which not only facilitate efficient ICT but also substantially enhance SOC, thereby markedly improving ISC efficiency and enabling effective utilization of triplet excitons. Molecular design strategies have led to breakthroughs in optimizing the lifetime, quantum yield, and color tunability of these materials. Studies demonstrate that incorporating rigid molecular frameworks and constructing intermolecular interaction networks can further enhance environmental stability and luminescence performance. With ongoing innovations in molecular design approaches, three-coordinate boron RTP materials show promising potential for broader applications in smart responsive materials and bioimaging fields.

2.2 Four-coordinate boron compounds

Four-coordinate compounds have shown significant value in the field of luminescent materials due to their unique electronic structure. The central boron of this type of compound is sp^3 hybridized, thus forming a tetrahedral configuration. Compared with three-coordinate boron, the occupation of its p_z orbital leads to a reduced electron acceptability, but it still retains certain electron-deficient characteristics. This special electronic structure makes it a key building block for the design of RTP materials.

Among various organic boron luminescent groups, the boron difluoride (BF_2) functional group has gained considerable attention due to its outstanding performance.[39,79,80] The difluoroboron β-diketonate complex, in particular, has emerged as one of the most widely used four-coordinate boron fluorescent dye systems owing to its large molar absorption coefficient and high fluorescence quantum yield.[81–90] Researchers have developed diverse four-coordinate boron complex systems by coordinating BF_2 with different heteroatoms. Through precise modulation of coordination atom electronegativity and substituent structures, the RTP properties of these materials can be finely tuned, providing valuable design principles for novel luminescent material development.

2.2.1 Difluoroboron β-diketonate derivatives. Difluoroboron β-diketonate derivatives have garnered significant research interest owing to their exceptional optical properties. These compounds are typically synthesized through Suzuki–Miyaura coupling reactions followed by cascade transformations involving aromatic ketones, carboxylic acids, trifluoroacetic anhydride, and boron trifluoride diethyl ether.[91] Table 3 shows the key photophysical parameters of the compounds in order of discussion: maximum wavelengths of fluorescence (λ_F) and phosphorescence (λ_P), lifetimes (τ_F and τ_P), and both phosphorescence and photoluminescence quantum yields (Φ_P and PLQY).

In 2007, Fraser *et al.* achieved a significant breakthrough by developing hydroxyl-functionalized difluoroboron dibenzoylmethane **55** (Fig. 7) as an initiator for synthesizing end-functionalized **56** *via* lactide ring-opening polymerization. Their study revealed that this material exhibits RTP characteristics with a lifetime of 0.17 s in the absence of oxygen, demonstrating metal-free phosphorescence emission at room temperature. The **56** system achieves efficient RTP solely through the polymer matrix's rigid confinement effect, which effectively suppresses non-radiative transitions of triplet excitons.[92]

Building upon these findings, researchers systematically modified difluoroboron β-diketonate derivatives to investigate the structure–RTP performance relationship. Xiao *et al.* maintained the core difluoroboron β-diketonate structure while introducing simple phenyl and methyl substituents without strong electron-donating/withdrawing groups, yet still observed RTP emission. Their study revealed that different solvent systems yielded two distinct crystal forms: yellow crystals (**57**-YG) from dichloromethane showed τ_P = 25.3 ms, while blue crystals (**57**-B) from *n*-hexane displayed much shorter τ_P = 92.4 μs. Single-crystal X-ray analysis demonstrated that although both crystals shared similar molecular configurations and packing modes, **57**-YG's stronger intermolecular interactions more effectively suppressed triplet exciton non-radiative decay, resulting in extended phosphorescence.[93] This work establishes that even minimal structural modifications can achieve superior phosphorescence through precise control of molecular packing, where subtle changes in intermolecular interactions may profoundly influence RTP performance.

In other studies, Wen *et al.* pursued an alternative approach by incorporating alkanol hydroxyl groups onto phenyl rings (**58**). By doping these derivatives in polystyrene (PS)/polyisoprene (PI) blends or PS–PI–PS(SIS) block copolymers, they achieved long-lived phosphorescence with τ_P = 310 ms and 630 ms, respectively. In this system, the PS matrix provides rigidity, while PI components function as oxygen barriers, with their synergistic effect effectively suppressing triplet exciton non-radiative transitions.[94]

Investigating heavy atom effects on phosphorescence properties, Ikeda *et al.* introduced iodine onto the phenyl group of the skeleton and observed that this derivative (**59**) displayed RTP characteristics exclusively in the crystalline state, exhibiting a phosphorescence lifetime of 1.3 ms.[95] These findings clearly demonstrate that while heavy atom incorporation enhances spin–orbit coupling (SOC), achieving efficient phosphorescence emission still necessitates a well-ordered molecular packing environment. Fraser *et al.* incorporated both phenyl and naphthalene groups into the difluoroboron β-diketonate framework (**60–63**) and systematically investigated how bromine substitution positions influence phosphorescence performance. Their comprehensive studies revealed that bromine substitution on the primary naphthalene moiety exerted the most pronounced effect on the emission lifetime. Surprisingly, the unsubstituted compound achieved an exceptionally long lifetime of 813 ms, whereas brominated derivatives showed substantially reduced lifetimes.[96] This initially counterintuitive observation can be rationalized by considering the dual role of bromine: while they indeed facilitate ISC through enhanced SOC, they simultaneously promote non-radiative decay pathways for triplet excitons, with the net result being an overall reduction in the observed phosphorescence lifetime.

In studies of unilateral modification systems, Fraser *et al.* demonstrated that RTP properties could be achieved through

Table 3 Photophysical properties of difluoroboron β-diketonate derivatives

Sample	Environment	λ_F [nm]	τ_F (ns)	λ_P [nm]	τ_P [ms]	Φ_P [%]	PLQY [%]	Ref.
55	Crystal	540	8.9	—	—	—	—	92
56	Film	440	1.2	509	170[a]	—	—	92
57	Crystal[b]	455	—	—	0.0924	14.1	28.1	93
57	Crystal[c]	521	—	530	25.3	—	39.1	93
58	1 wt% in PS	410	—	—	—	—	—	94
58	In PI	—	—	—	—	—	—	94
58	5 wt% in PS and PI	443	—	500	310	—	—	94
58	0.1 wt% in SIS	410	3.37	500	630	12.9	—	94
59	Crystal	460	4.0	527	1.3	—	25.0	95
60	1.3 wt% in PLA	444	3.29	541	813	—	—	96
61	1.3 wt% in PLA	437	0.78	554	13.6	—	—	96
62	1.3 wt% in PLA	449	2.52	544	341	—	—	96
63	1.3 wt% in PLA	448	0.75	561	12.9	—	—	96
64	1 wt% in PLA	389	0.5	489	255	—	—	97
65	1 wt% in PLA	438	5.09	543	270	—	—	97
66	1 wt% in PLA	438	2.75	567	295	—	—	97
67	1 wt% in PLA	420	3.34	452	113	—	—	97
68	0.1 wt% in PhB powder	437	—	421[d] 483[e]	302.6[d] 328.6[e]	—	16.5	98
69	0.1 wt% in PhB powder	432	—	421[d] 474[e]	278.2[d] 297.9[e]	—	9.4	98
70	0.1 wt% in PhB powder	434	—	424[d] 465[e]	180.1[d] 286.2[e]	—	12.4	98
71	1 wt% in SCS	455	—	523	151.8	—	3.09	99
72	0.5 wt% in SCS	459	—	533	260	—	3.12	99
73	0.5 wt% in SCS	442	—	525	265.2	—	3.21	99
74	0.001 wt% in PhB	463	—	463[f]	199[f]	—	—	91
75	0.01 wt% in PhB	425	—	514	1015	—	—	91
76	0.001 wt% in PhB	442	—	442[f]	315.3[f]	—	24.7	91
77	0.01 wt% in PhB	455	—	456[f]	345.1[f]	—	30.9	91
78	0.01 wt% in PhB	422	—	522	1079	—	—	91
79	In PMMA/wood	414	—	524	1023.9	—	29	100
79	In PMMA	409	—	520	805.3	—	—	100
80	In PMMA/wood	408	—	515	1053.3	—	35	100
80	In PMMA	407	—	514	942.5	—		100
81	81/TMB 0.2 wt% in PhB	463	—	463[g]	—	—	51.0	101
82	82/TMB 0.2 wt% in PhB	463/490	7.9	465/496[g]	—	—	17.7	101
83	83/TMB 0.2 wt% in PhB	472/483	6.0	470/492[g]	—	—	11.4	101
84	84/TMB 0.2 wt% in PhB	463/493	2.4	463/495[g]	—	—	7.3	101
85	85/TMB 0.2 wt% in PhB	471/496	2.8	468/498[g]	—	—	2.1	101
86	86/TMB 0.5 wt% in MeOPhB	503	—	503[g]	—	—	16.6	102
87	87/TMB 0.5 wt% in MeOPhB	500	—	508[g]	—	—	21.9	85
87	87/TMB 0.2 wt% in MeOPhB	499	—	505[g]	—	—	—	85
88	88/TMB 0.3 wt% in MeOPhB	472/493	—	497[g]	—	—	19.5	85
88	88/TMB 0.2 wt% in MeOPhB	473	—	494[g]	—	—	—	85
89	89/TMB 0.3 wt% in MeOPhB	474	—	495[g]	—	—	20.8	85
89	89/TMB 0.2 wt% in MeOPhB	472/491	—	473[g]	—	—	—	85
90	0.05 wt% in PhB	439	8.28	466	284	—	9.6	103
91	0.05 wt% in PhB	433	14.10	—	—	—	—	103
92	0.05 wt% in PhB	436	5.25	—	—	—	—	103
93	0.05 wt% in PhB	436	3.84	484	221	—	—	103
94	0.05 wt% in PhB	421	2.08	514	1046	—	9.2	103
95	In BP	483	—	531	115.3	3.0	5.8	104
96	In BP	480	—	542	360.3	15.9	18.3	104
97	In BP	498	—	553	523.8	4.1	8.9	104
98	In BP	565	—	652	159.3	0.8	3.2	104

[a] Measured in the absence of oxygen. [b] **57**-B (blue). [c] **57**-YG (yellow). [d] Dual phosphorescence: T_n, $n \geq 2$, $n = 2$ for **68**-PhB and **69**-PhB materials and $n = 3$ for the **70**-PhB material. [e] Dual phosphorescence: T_1. [f] Emission wavelength of thermally activated delayed fluorescence. [g] Emission wavelength of OLPL. Abbreviations: PS: polystyrene, PI: polyisoprene, SIS: PS–PI–PS, PLA: polylactic acid, PhB: phenyl benzoate, SCS: silkworm cocoon silk, TMB: *N*,*N*,*N*′,*N*′-tetramethylbenzidine; MeOPhB: 4-methoxyphenyl benzoate, and BP: benzophenone.

modification of just one side of the difluoroboron β-diketonate skeleton. Their systematic investigation involved designing a series of single-phenyl-methoxy-substituted derivatives (**64–67**), through which they achieved precise modulation of phosphorescence performance by controlling both the number (ranging from 1 to 3) and the positional arrangement (*para*, *meta*, and *ortho*) of methoxy groups. When incorporated into PLA matrices, these derivatives exhibited phosphorescence lifetimes between 113 and 295 ms, with tunable emission colors spanning from blue to yellow.[97]

Building upon this foundation, Zhang *et al.* developed a novel molecular design incorporating both methoxy and

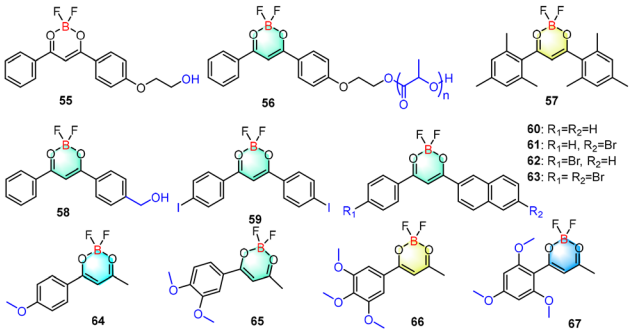

Fig. 7 Difluoroboron β-diketonate derivatives (I) (compounds **55–67**).

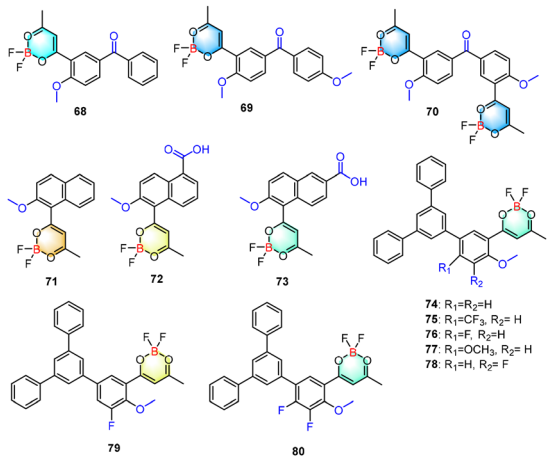

Fig. 8 Difluoroboron β-diketonate derivatives (II) (compounds **68–80**).

benzophenone groups onto the framework (**68–70**) (Fig. 8) and doped **68** into phenyl benzoate (PhB) matrices, observing in this system an unusual phosphorescence phenomenon that appeared to violate Kasha's rule.[98] Further advancing this research direction, the same group subsequently engineered a composite phosphorescent material based on natural silkworm cocoon silk by introducing multiple functional groups (including naphthalene, methoxy, and carboxyl moieties) (**71–73**) onto one side of the difluoroboron β-diketonate skeleton. This innovative design yielded remarkable enhancements in phosphorescence performance, achieving an extended lifetime of 265.2 ms while simultaneously improving the material's biocompatibility.[99] In parallel developments, Zhang *et al.* investigated the effects of incorporating fluorine and methoxy groups into the difluoroboron β-diketonate skeleton (**74–78**) followed by doping in PhB, observing phosphorescence lifetimes more than 1000 ms.[91] Their subsequent structural optimization involved the introduction of additional fluorine (**79** and **80**) to strengthen intermolecular hydrogen bonding, ultimately producing an ultralong phosphorescent material with exceptional performance (τ_P = 1035.3 ms) when embedded in PMMA/wood matrices. This advanced material system combines outstanding optical transparency (>90%) with practical functionalities including oil resistance, anti-fingerprint properties, and waterproof characteristics, highlighting its significant potential for various applications.[100]

In their systematic research studies, Zhang *et al.* discovered that phenylmethoxy-modified difluoroboron β-diketonate skeletons could maintain excellent RTP performance even after further introduction of additional functional groups. In accordance with the unilateral modification strategy, the researchers developed a series of difluoroboron β-diketonate derivatives **81–85** (Fig. 9) with ICT characteristics by introducing phenyl groups at the *para* position of benzoxy groups and attaching various atoms to these phenyl groups. These compounds exhibited S_1 states with substantial dipole moments, enabling effective regulation of singlet–triplet energy gaps through dipole interactions with the PhB matrix. Their studies revealed that when using hydrogen-substituted phenyl groups (**81**-PhB system) combined with the electron donor *N*,*N*,*N*′,*N*′-tetramethylbenzidine (TMB) as a third component, the system demonstrated organic long-persistent luminescence (OLPL) lasting several hours, as the TMB electron donor facilitated charge separation and established a dual afterglow mechanism to significantly prolong emission duration.[101] Expanding on this work, Zhang *et al.* successfully incorporated phenylene ether structures into the phenylmethoxy groups attached to difluoroboron β-diketonate (**86**), constructing a three-component system with a 4-methoxyphenyl benzoate (MeOPhB) matrix and a TMB electron donor which achieved OLPL afterglow persisting for up to 2 hours.[102] Further systematic investigations by Zhang *et al.* examined the effects of introducing naphthalene groups at the *para* position of phenylmethoxy groups (**87–89**), using MeOPhB as the matrix and TMB as the electron donor, with the modified system exhibiting a remarkably extended afterglow duration of 2.5 hours.[85] These groundbreaking findings not only highlight the tremendous potential of ultralong afterglow materials but also provide crucial theoretical guidance and innovative design principles for developing high-performance RTP systems. Through meticulous molecular engineering and precise component optimization, this research has significantly improved the luminescence properties of organic materials, establishing novel pathways for the development of organic long-persistent luminescent materials with exceptional performance characteristics.

Zhang *et al.* demonstrated that the unilateral heavy atom effect could also achieve excellent RTP performance (**90–94**). Their studies showed that in the phenyl benzoate (PhB) matrix, the iodine-substituted difluoroboron β-diketonate compound (**94**) exhibited an exceptionally long RTP lifetime reaching 1.0 s,

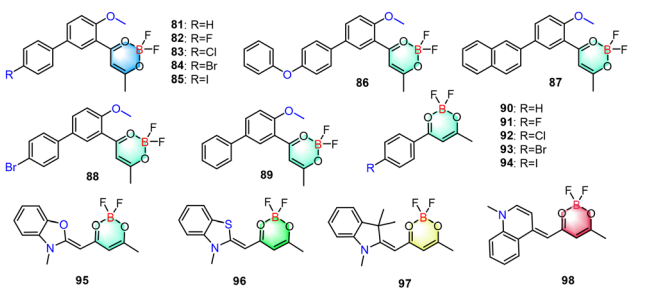

Fig. 9 Difluoroboron β-diketonate derivatives (III) (compounds **81–98**).

representing one of the longest lifetimes reported for iodine-containing organic RTP systems.[103]

Sun *et al.* addressed the color limitation in these materials through innovative structural modifications. Their research demonstrated that introducing heterocyclic structures into the side chains of the skeleton (**95–98**) and doping them into the benzophenone (BP) matrix enabled full-color phosphorescence tuning from emerald green to red while maintaining long lifetimes up to 523.8 ms when doped in PhB.[104] This breakthrough provides a novel strategy for developing panchromatic phosphorescent materials with tunable emission colors.

Difluoroboron β-diketonate derivatives have been successfully developed into high-performance RTP systems exhibiting long lifetimes (>1000 ms) and multicolor luminescence through strategic modifications including unilateral/bilateral functionalization and crystallization engineering, demonstrating significant application potential. Through systematic research of the structure–property relationships, researchers anticipate that the performance of these materials can be further optimized in future studies.

2.2.2 Other four-coordinate boron compounds. Based on the excellent RTP properties of difluoroboron β-diketonates, researchers have explored structural modifications by replacing the two oxygen atoms in the OOBF framework with heteroatoms of varying electronegativity (O/N/S/C), which significantly alters the RTP characteristics. Through this systematic heteroatom substitution strategy, researchers have successfully achieved precise control over the luminescence properties of these materials. Table 4 shows the key photophysical parameters of the compounds in order of discussion: maximum wavelengths of fluorescence (λ_F) and phosphorescence (λ_P), lifetimes (τ_F and τ_P), and both phosphorescence and photoluminescence quantum yields (Φ_P and PLQY).

The original difluoroboron β-diketonate system exhibited excellent phosphorescence properties due to its two highly electronegative O atoms coordinated to the boron center. When researchers substituted one O atom with a N atom of slightly lower electronegativity, they observed significant changes in RTP performance. Neelakandan *et al.* synthesized a naphthalidenimine–boron compound with a simple skeleton containing

Table 4 Photophysical properties of other four-coordinate boron compounds

Sample	Environment	λ_F [nm]	τ_F (ns)	λ_P [nm]	τ_P [ms]	Φ_P [%]	PLQY [%]	Ref.
99	99@4,4′-Dimethoxy benzophenone	496	—	557	1.49	—	—	105
100	Green crystal	514	0.56	558	—	—	26 ± 1	106
100	Red crystal	505	0.41	598	0.009	—	2.8 ± 1	106
101	In CH_2Cl_2	501	2.07	568	0.001	—	29	107
102	In CH_2Cl_2	500	1.69	558	0.005	—	86	107
103	In CH_2Cl_2	470	2.94	599	0.001	—	104	107
104	In CH_2Cl_2	478	3.77	588	0.003	—	100	107
105	In CH_2Cl_2	493	2.07	621	0.001	—	70	107
106	In CH_2Cl_2	537	4.79	653	0.002	—	98	107
107	In CH_2Cl_2	483	4.73	606	0.003	—	49	107
108	In CH_2Cl_2	515	7.6 ± 0.2	—	—	—	90	108
108	In CH_2Cl_2	—	—	—	—	—	—	109
109	In CH_2Cl_2	—	—	575	0.008	—	10	108
109	In CH_2Cl_2	—	—	—	0.024[a]	—	—	109
					0.008[b]	—		
110	In CH_2Cl_2	—	—	545	0.009	—	—	109
111	In CH_2Cl_2	554	0.97	—	—	—	—	110
111	Powder	550	0.32	—	—	—	—	110
111	Doped crystal	510	0.29	605	1.57	13.43	—	110
112	In CH_2Cl_2	525	0.26	—	—		—	110
112	Powder	528	0.35	—	—		—	110
112	Doped crystal	512	0.31	611	0.83	15.96	—	110
113	Solid	500	0.135	662	0.107	0.2	—	111
114	Solid	485	0.217	646	0.100	0.3	—	111
115	Solid	496	0.186	661	0.165	0.3	—	111
116	Solid	484	0.134	666	0.189	0.6	—	111
117	1 wt% in PMMA	537[c]	—	567[c]	0.00191	—	28[d]	112
117	G-crystal	530[c]	—	541[c]	—	—	58[d]	112
117	Y-crystal	—	—	570[c]	0.00047[c]	—	77[d]	112
117	R-crystal	630[c]	—	633[c]	—	—	23[d]	112
118	Pure film	401	—	478	3.8	0.1	30	113
118	Crystal	410	—	515	12.0	1.8	23	113
119	Pure film	413	—	588	2.7	<0.1	12	113
119	Crystal	412	—	440[e]	3.9	0.1[f]	16	113
				565	8.2			
120	Pure film	487	—	592	3.0	<0.1	22	113
120	Crystal	502	—	580	11.4	<0.1	9	113

[a] Calculated value. [b] Experimental value. [c] The fluorescence and phosphorescence emission peaks are confirmed by the time-resolved PL spectra at 50 K. [d] Measured at room temperature under Ar. [e] The peak at 440 nm is consistent with delayed fluorescence *via* triplet–triplet annihilation. [f] The quantum yield provided is a combination of both long-lived photoluminescence events that could not be resolved from one another due to their similar lifetimes.

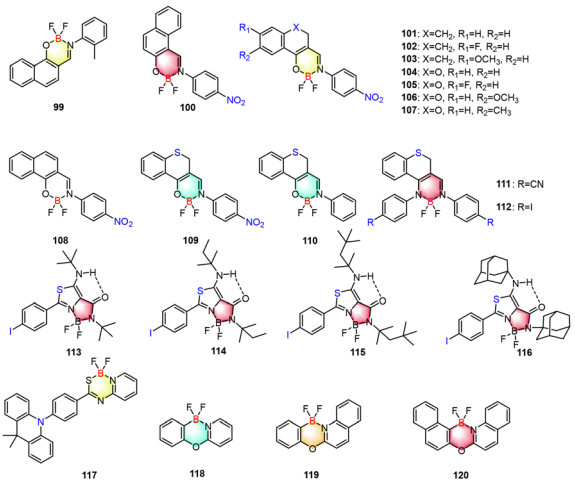

Fig. 10 Other four-coordinate boron compounds (**99–120**).

only naphthalene, phenyl and methyl groups (**99**) (Fig. 10), which was coated on 4,4′-dimethoxybenzophenone crystals. Their study revealed that FRET occurred in this system due to the spectral overlap between donor emission and acceptor absorption, resulting in yellow-green phosphorescence with a lifetime of 1.49 ms,[105] demonstrating how N substitution enhances phosphorescence through strengthened intermolecular interactions. Fu *et al.* further modified the system by replacing the methyl group with a more electron-withdrawing nitro group to enhance the ICT effect, creating a boron difluoride β-acetylnaphthalene chelate (**100**) that formed two distinct crystal forms: green crystals exhibiting J-aggregation and TADF, and red crystals showing H-aggregation and RTP properties.[106] These findings not only confirmed heteroatom substitution's regulatory effect on phosphorescence but also achieved controllable switching between TADF and RTP through aggregation state engineering. Venkatesan *et al.* successfully optimized the phosphorescence performance of compounds by introducing oxygen-containing heterocyclic structures into the N,O-substituted difluoroboron molecular framework and precisely modulating the electronic effects of electron-withdrawing and electron-donating groups (**101–107**).[107] Building upon this foundation, Fu *et al.* further advanced this design strategy. By replacing carbon atoms with sulfur atoms, they designed and synthesized novel difluoroboron compounds (**108–109**). Theoretical calculations and experimental studies demonstrated that the lone pair electrons of sulfur atoms and nitro groups generate a significant ICT effect, substantially enhancing the ISC efficiency. This innovative design endowed S-BF_2 with phosphorescence properties in solution that were absent in its carbon-substituted counterpart, achieving a phosphorescence lifetime of 8.3 ms.[108] Subsequently, Huang *et al.* (**108–110**) further elucidated the mechanism of sulfur-containing heterocycles through more in-depth theoretical research. They found that sulfur atoms not only participate in the ICT process through their lone pair electrons but also significantly enhance SOC effects *via* their empty d-orbitals, thereby improving ISC rates. Additionally, the introduction of sulfur atoms suppressed out-of-plane molecular twisting motions, effectively reducing non-radiative decay rates.[109] Although the RTP lifetimes of these compounds remain at the microsecond level, these studies systematically revealed the multiple roles of sulfur-containing heterocycles in regulating phosphorescence performance: they can both accelerate ISC through n → π* transitions and inhibit non-radiative decay by enhancing molecular rigidity.

Fu *et al.* replaced oxygen atoms in the molecule with nitrogen atoms and introduced either heavy-atom-effect-exhibiting diiodo groups or cyano groups capable of promoting intramolecular charge transfer (**111** and **112**). By using 4-iodoaniline (I–Ph–NH_2) crystals as a host matrix for doping, they successfully achieved highly efficient room temperature phosphorescence (RTP).[110] Zhu *et al.* further advanced the work by designing and synthesizing *N*,*N*-chelated compounds (**113–116**). Their research demonstrated that varying alkyl substituent sizes could modulate RTP properties. Crystal structure analyses revealed that halogen bonding involving iodine atoms and C–H···π interactions effectively stabilized the triplet state, enabling dual emission in both amorphous and crystalline states.[111]

Investigating the influence of electronegativity on RTP performance, Wang *et al.* developed an N, S-complex by substituting O with S atoms from the same group. They designed a four-coordinate structure **117**, using 9,10-dihydro-9,9-dimethylacridine (DMAC) as the donor (D) and N,S-thioamide difluoroboron as the acceptor (A). Their study revealed that among the three resulting crystal forms, the yellow crystal exhibited a larger ΔE_{ST}, effectively suppressing reverse intersystem crossing (RISC). Furthermore, the heavy atom effect of sulfur enhanced SOC, leading to prominent RTP characteristics in this crystal, while the other two crystals primarily displayed TADF behavior.[112]

While previous studies primarily relied on heavy atom effects with limited phosphorescent color tunability, Gilroy *et al.* developed an alternative approach using C atoms (with lower electronegativity than N/S) in four-coordinate boron (BF_2) systems (**118–120**). Their work demonstrated that efficient RTP could be achieved through interactions among light atoms (O, F, *etc.*) without heavy atom involvement. As the conjugated system expanded, the phosphorescence emission color systematically varied.[113] This light-atom-interaction strategy for high-efficiency RTP avoids the toxicity issues associated with heavy atoms while enabling color tunability, opening new possibilities for RTP material development.

Researchers have successfully achieved efficient RTP performance and color tunability by systematically substituting atoms with varying electronegativity (from highly electronegative O to progressively less electronegative N, S, and C atoms) in these systems. These accomplishments fundamentally rely on the pivotal role of the BF_2 core. The electronegativity-based design strategy established through these studies provides valuable insights and expanded possibilities for developing other organic RTP materials in future research.

Although many BF_2-bridged β-diketonate complexes have been reported, their photophysical behavior varies significantly:

some show fluorescence, while others exhibit RTP. This indicates that the BF_2 unit alone does not guarantee RTP and its luminescence depends strongly on molecular design and environmental conditions. Several strategies have been developed to promote RTP. Host–guest doping is widely used to suppress non-radiative decay and enhance phosphorescence by careful selection of host materials and optimization of doping conditions. At the molecular level, introducing heavy atoms (*e.g.*, Br and I) strengthens SOC to improve ISC and quantum yield. Heteroatom substitution (*e.g.*, S and O) can tune energy levels and singlet–triplet gaps to facilitate RTP. Additionally, ICT systems help stabilize triplet excitons and create new radiative pathways, increasing phosphorescence intensity and lifetime. These approaches highlight that RTP relies on multi-factor synergy. Future work should focus on mechanistic studies of excited-state processes to enable more rational material design.

Four-coordinate boron compounds exhibit remarkable design flexibility and tunable performance in RTP materials owing to their characteristic sp^3-hybridized tetrahedral geometry and electron-deficient nature. The difluoroboron β-diketonate derivatives, as representative structures of this system, have achieved ultra-long phosphorescence lifetimes up to 1035.3 ms through synergistic effects between rigid molecular frameworks and optimized intermolecular interactions. Researchers have successfully implemented precise control over both the phosphorescence lifetime and the emission color through strategic single/bilateral substitution patterns. Efficient RTP emission has been realized by suppressing non-radiative transitions *via* crystallization engineering and host–guest doping strategies, while ISC efficiency has been further enhanced through heteroatom substitution (O/N/S/C) and heavy-atom effects. Future research will concentrate on enhancing quantum yields and broadening the spectral range of luminescent colors in these materials.

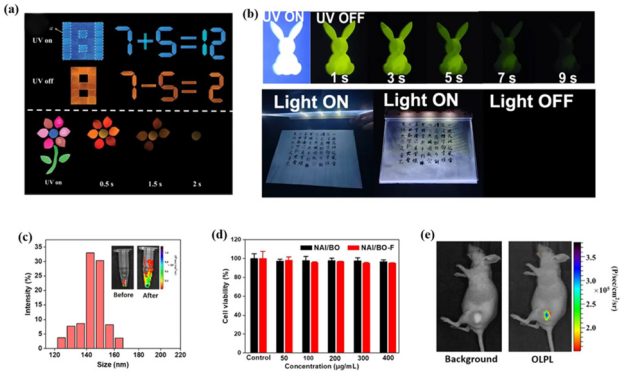

Fig. 11 (a) Information encryption applications of **48** films. The flower core is made of the **48**@PMMA film; petal ①, petal ②, and petal ③ are made of **48**/RhB@PMMA films, **48**/Rh6G@PMMA films, and **48**/RBNN@PMMA films, respectively; and the flower branches and leaves are made of **47**@PMMA films. Reproduced with permission from ref. 74. Copyright 2024 Advanced Functional Materials. (b) Rabbit patterns of **79**/wood afterglow materials (top); a commercial flat-panel night reading light (bottom). Reproduced with permission from ref. 100. Copyright 2025 Nature Communications. (c) Size distribution of NAI-BO-F (1 mg mL^{-1}). Inset: Phosphorescence images of nanoparticles (1 mg mL^{-1}) before and after F127 encapsulation. (d) 4T1 cell viability at different concentrations of NAI/BO-F. (e) Phosphorescence imaging of mice subcutaneously injected with NAI/BO-F (0.1 mg mL^{-1}). Reproduced with permission from ref. 56. Copyright 2025 Advanced Materials.

3. Applications

Boron-based RTP materials demonstrate excellent phosphorescence properties while offering tunable emission colors and prolonged lifetimes through strategic modifications of boron's numbers and substituent types. These materials show significant potential for various applications including anti-counterfeiting technologies, light-emitting displays, and biological imaging systems.

3.1 Anti-counterfeiting/information encryption

Our research group has systematically investigated triarylborane compounds and successfully developed a series of derivatives exhibiting outstanding RTP characteristics. Building upon these materials' unique luminescent properties, we have designed and demonstrated novel anti-counterfeiting encryption applications with enhanced security features (Fig. 11(a)). In our experimental design, we creatively employed the distinct RTP behaviors of **48** in different matrices to develop advanced anti-counterfeiting systems. By depositing **48** onto filter paper using DCM solution and preparing PMMA films, we constructed a square pattern and the equation "7 + 5 = 12," respectively. The system demonstrates dynamic information encryption as **48**@filter paper shows no RTP, while the **48**@PMMA film exhibits strong RTP under UV light, causing the square to transform into "8" and the equation to change from "7 + 5 = 12" to "7–5 = 2". To further validate the material's anti-counterfeiting capabilities, we designed an intricate flower pattern incorporating **48**@PMMA with various fluorescent dyes in different petal sections. The differential afterglow durations of these components create a time-dependent anti-counterfeiting effect, where petals appear to wither sequentially as their luminescence gradually fades after UV excitation.[74]

3.2 Light-emitting display

Boron-based RTP materials, characterized by their exceptionally prolonged luminescence lifetimes, exhibit considerable promise for advanced lighting and display applications. Zhang *et al.* showed that difluoroboron β-diketonate derivatives, RTP materials, can be processed *via* multiple methods for functional implementations, including fabrication into various geometric forms or incorporation into wood substrates to create night lights (Fig. 11(b)). Through molecular design and host–guest doping strategies, their team achieved remarkable afterglow durations extending up to 2.5 hours, substantially expanding the lighting and display applications of RTP materials.[100] These ultra-long afterglow characteristics position them as ideal lighting materials that offer environmental advantages and energy efficiency compared to conventional LED technologies.

3.3 Biological imaging

Boron-based RTP materials have demonstrated groundbreaking applications in the biomedical field. Lin *et al.* developed an

NAI/BO composite through solid-phase thermal treatment using BA as the matrix and 2,3-naphthyldiformimide (NAI), which exhibited exceptional OLPL properties lasting up to 3 hours. To enhance stability, the group further engineered NAI/BO-F nanoparticles by encapsulating NAI/BO with amphiphilic copolymer F127 (Fig. 11(c)). Following subcutaneous injection of UV-activated NAI/BO-F nanoparticles into Balb/c nude mice, distinct OLPL signals were successfully observed using an IVIS *in vivo* imaging system (Fig. 11(d) and (e)). The material's significantly longer OLPL lifetime compared to biological autofluorescence effectively eliminates background interference, enabling high signal-to-noise ratio bioimaging. This innovative "*ex vivo* activation–*in vivo* imaging" approach[56] overcomes the limitations of conventional fluorescence imaging that requires continuous excitation, establishing a novel technical pathway for biomedical imaging applications.

Although boron-based RTP materials show great application potential in fields such as anti-counterfeiting, displays, and bioimaging, their practical industrialization still faces several critical challenges. Firstly, the stability of the materials in aqueous solution remains a major issue. It should be specifically noted that this challenge is particularly pronounced for boronic acid (BA)-based RTP materials due to the inherent hydrolytic susceptibility of the boronic acid functional group. While some four-coordinate boron complexes demonstrate relatively better water stability, most current boron-based RTP materials are prone to hydrolysis in water, and their luminescence properties are significantly affected by pH, necessitating the development of novel water-stable boron coordination structures. Secondly, in terms of spectral regulation, although full spectral coverage from 400 nm to 650 nm has been achieved, luminescence performance in the near-infrared region (650–900 nm) still requires breakthrough improvements, which will directly affect their application value in OLEDs and deep-tissue imaging. Furthermore, many problems exist in device integration, as the technology in this area remains immature compared to theoretical research. In the biomedical field, systematic toxicity evaluation systems are not yet well-established, highlighting the need to standardize biocompatibility testing protocols and develop metabolizable boron-based RTP materials. Looking ahead, future development should focus on molecular engineering to create near-infrared luminescent systems, explore smart responsive RTP materials, and develop water-soluble modification strategies to enhance biocompatibility. These efforts will strongly promote the practical application of boron-based RTP materials.

4. Summary and perspectives

This study systematically reviews the recent advances in three- and four-coordinate boron RTP materials. Owing to their structural tunability, multicolor phosphorescence, processability, and multi-stimuli responsiveness, these materials demonstrate broad application potential in anti-counterfeiting, light-emitting displays, and biological imaging. By precisely modulating the coordination type of boron atoms and the number, type, and position of substituents and designing host–guest doping systems, researchers have successfully achieved long-lived RTP and full-color phosphorescence emission, providing key insights for the development of novel functional materials.

Research has demonstrated that boron coordination modes significantly influence material luminescence mechanisms and properties. Three-coordinate boron typically exhibits higher phosphorescence quantum yields owing to stronger π-conjugation effects, while four-coordinate boron shows relatively lower quantum yields. Nevertheless, the latter can achieve excellent RTP performance through molecular design. These differences originate from how coordination modes regulate the molecular structure, SOC, and non-radiative transition processes. Substituent modification represents another crucial approach for tuning boron-based RTP materials. Compared to simple boric acid compounds, phenylboronic acid's p–π conjugation effect markedly enhances ISC efficiency, and triarylboranes demonstrate superior RTP properties through synergistic effects of three aromatic groups. The introduction of electron-donating groups (*e.g.*, methoxy and dimethylamino) and polycyclic aromatic hydrocarbons (*e.g.*, naphthalene and benzoperylene) enables further modulation of the emission color and lifetime. Notably, heavy atom effects in boron-based RTP systems present an intriguing phenomenon: while enhancing SOC, they sometimes reduce the lifetime, revealing the complex balance required between SOC promotion and non-radiative transition suppression in RTP molecular design. Regarding host–guest strategies, BA's rigid structure and oxygen barrier properties significantly improve guest molecule RTP performance. Moreover, optimizing host–guest ratios enables precise control of the emission color and lifetime, demonstrating this approach's strong regulatory potential.

Compared to traditional organic RTP material systems, boron-based RTP materials demonstrate outstanding comprehensive performance advantages: in terms of luminescence properties, their maximum phosphorescence quantum yield exceeds 45%, significantly surpassing that of conventional systems (typically $<20\%$); regarding luminescence kinetics, particularly three-coordinate organoboron compounds generally achieve phosphorescence emission with a long lifetime on the order of seconds; in spectral tunability, precise molecular engineering enables coverage across the entire visible range of 400–650 nm, with effective realization of long-wavelength emission. Especially notable are the RTP systems constructed based on boric acid (BA), which combine excellent biocompatibility. This unique synergy of "high performance and low toxicity" renders them irreplaceable for biomedical applications. These characteristics make boron-based RTP materials highly valuable for use in fields such as anti-counterfeiting, displays, and bioimaging.

In summary, this review systematically examines recent advances in boron-based RTP materials, particularly focusing on structure–property relationships. Through precise regulation of boron coordination types (three- and four-coordinate), substituent characteristics (number, type, and position), heavy atom effects, diboron frameworks, and host–guest doping strategies, researchers have achieved remarkable progress extending phosphorescence lifetimes from microseconds to seconds, expanding

emission colors from single green/yellow to full-spectrum coverage, and significantly enhancing quantum yields. These accomplishments have established a comprehensive theoretical framework for designing high-performance boron-based RTP materials.

While boron-based RTP materials have achieved significant research breakthroughs, several challenges persist. Future research should focus on (i) deeper investigation of structure–property relationships to enable more efficient RTP performance through molecular design, particularly for four-coordinate boron compounds where low phosphorescence quantum yields remain problematic; (ii) overcoming the water stability limitations of BA matrices that currently restrict biological imaging applications to nanomaterial composites; (iii) advancing practical applications to fully realize the potential of these materials; (iv) expanding the color gamut, especially achieving efficient and stable blue-emitting and near-infrared (NIR) RTP materials, which are crucial for full-color displays and deep-tissue bioimaging; and (v) exploring intelligent applications, such as stimuli-responsive smart systems and adaptive optical devices that react dynamically to environmental changes. These efforts will require continuous exploration of novel material systems and application strategies.

Author contributions

Siying Peng designed the review framework and drafted the review. Xueqi Cai systematically organized the relevant literature. Qiuyu Zhang arranged and organized the figures. Yitong Sun, Liyan Zheng, and Qiue Cao contributed to revising the manuscript. Yonggang Shi oversaw the entire project, from review topic selection to manuscript completion.

Conflicts of interest

There are no conflicts to declare.

Data availability

This is a review article and no new data were generated. All cited data are available in the referenced published literature.

Acknowledgements

This work was financially supported by the National Natural Science Foundation of China (NSFC, 22565036, 21901225, 21964020, and 22164020), the Yunnan Fundamental Research Projects (202501AT070223 and 202301AT070406), and the Yunnan Revitalization Talent Support Program (C6213001212).

Notes and references

1 W. Gao, D. Li, H. Feng and Z. Su, Stretchable organic room temperature phosphorescence systems, *J. Mater. Chem. C*, 2025, **13**, 13607–13619.
2 Y. Yang, Q. Li and Z. Li, Advances in organic room-temperature phosphorescence: design strategies, photophysical mechanisms, and emerging applications, *Mater. Chem. Front.*, 2025, **9**, 744–753.
3 H. Li, Z. Xue, G. Yang, F. Meng, H. Lin, W. Zhao, S. Chen and C. Wang, Pyrene-based, red-emitting, aggregation-induced emission luminogens: from structural construction to anti-counterfeiting applications, *Mater. Chem. Front.*, 2025, **9**, 318–324.
4 M. Ji and X. Ma, Recent progress with the application of organic room-temperature phosphorescent materials, *Ind. Chem. Mater.*, 2023, **1**, 582–594.
5 W. Xu, B. Wang, S. Liu, W. Fang, Q. Jia, J. Liu, C. Bo, X. Yan, Y. Li and L. Chen, Urea-formaldehyde resin room temperature phosphorescent material with ultra-long afterglow and adjustable phosphorescence performance, *Nat. Commun.*, 2024, **15**, 4405.
6 D. Ma, Z. Li, K. Tang, Z. Gong, J. Shao and Y. Zhong, Nylons with Highly-Bright and Ultralong Organic Room-Temperature Phosphorescence, *Nat. Commun.*, 2024, **15**, 4402.
7 Y. Zhang, H. Li, M. Yang, W. Dai, J. Shi, B. Tong, Z. Cai, Z. Wang, Y. Dong and X. Yu, Organic room-temperature phosphorescence materials for bioimaging, *Chem. Commun.*, 2023, **59**, 5329–5342.
8 Kenry, C. Chen and B. Liu, Enhancing the performance of pure organic room-temperature phosphorescent luminophores, *Nat. Commun.*, 2019, **10**, 2111.
9 Z. Yin, Z. Wu and B. Liu, Recent Advances in Impurity-Induced Room-Temperature Phosphorescence, *Adv. Mater.*, 2025, 2506549.
10 Y. Zhao, J. Yang, C. Liang, Z. Wang, Y. Zhang, G. Li, J. Qu, X. Wang, Y. Zhang, P. Sun, J. Shi, B. Tong, H. Y. Xie, Z. Cai and Y. Dong, Fused-Ring Pyrrole-Based Near-Infrared Emissive Organic RTP Material for Persistent Afterglow Bioimaging, *Angew. Chem., Int. Ed.*, 2023, **63**, e202317431.
11 Z. Wu, H. Choi and Z. M. Hudson, Achieving White-Light Emission Using Organic Persistent Room Temperature Phosphorescence, *Angew. Chem., Int. Ed.*, 2023, **62**, e202301186.
12 F. Liao, J. Du, X. Nie, Z. Wu, H. Su, W. Huang, T. Wang, B. Chen, J. Jiang and X. Zhang, Modulation of red organic room-temperature phosphorescence in heavy atom-free phosphors, *Dyes Pigm.*, 2021, **193**, 109505.
13 H. Yao, F. Yang, J. Hu, W. Cao, S. Qin, T.-B. Wei, B. Shi and Q. Lin, Ultralong room temperature phosphorescence and broad color-tunability persistent luminescence *via* new strategy, *Chin. Chem. Lett.*, 2025, **36**, 110375.
14 R. Liang, L. Huo, A. Yu, J. Wang, C. Jia and J. Li, A micro-wave strategy for synthesizing room temperature phosphorescent materials, *Chin. Chem. Lett.*, 2022, **33**, 243–246.
15 K. Li, X. Qi, F. Li, Y. Xie, L. Zhang and Z. Li, ''Strong Assisting Weak'' Effect for Long-Lived Room Temperature Phosphorescence in Host–Guest-Doped Systems, *Angew. Chem., Int. Ed.*, 2025, e202508587.
16 F. Ma, B. Wu, S. Zhang, J. Jiang, J. Shi, Z. Ding, Y. Zhang, H. Tan, P. Alam and J. W. Lam, Lone pairs-mediated multiple

through-space interactions for efficient room-temperature phosphorescence, *J. Am. Chem. Soc.*, 2025, **147**, 10803–10814.
17 H. Zhu, J. Liu, Y. Wu, L. Wang, H. Zhang, Q. Li, H. Wang, H. Xing, J. L. Sessler and F. Huang, Substrate-responsive pillar [5] arene-based organic room-temperature phosphorescence, *J. Am. Chem. Soc.*, 2023, **145**, 11130–11139.
18 W. Zhao, Z. He and B. Z. Tang, Room-temperature phosphorescence from organic aggregates, *Nat. Rev. Mater.*, 2020, **5**, 869–885.
19 Z. Cong, M. Han, Y. Fan, Y. Fan, K. Chang, L. Xiao, Y. Zhang, X. Zhen, Q. Li and Z. Li, Ultralong blue room-temperature phosphorescence by cycloalkyl engineering, *Mater. Chem. Front.*, 2022, **6**, 1606–1614.
20 J. Zhou, L. Stojanović, A. A. Berezin, T. Battisti, A. Gill, B. M. Kariuki, D. Bonifazi, R. Crespo-Otero, M. R. Wasielewski and Y.-L. Wu, Organic room-temperature phosphorescence from halogen-bonded organic frameworks: hidden electronic effects in rigidified chromophores, *Chem. Sci.*, 2021, **12**, 767–773.
21 Z. Wu, J. Nitsch and T. B. Marder, Persistent room-temperature phosphorescence from purely organic molecules and multi-component systems, *Adv. Opt. Mater.*, 2021, **9**, 2100411.
22 J. Guo, C. Yang and Y. Zhao, Long-lived organic room-temperature phosphorescence from amorphous polymer systems, *Acc. Chem. Res.*, 2022, **55**, 1160–1170.
23 H. Sun, S. Shen and L. Zhu, Photo-stimuli-responsive Organic Room-Temperature Phosphorescent Materials, *ACS Mater. Lett.*, 2022, **4**, 1599–1615.
24 W. Wang, Y. Zhang and W. J. Jin, Halogen bonding in room-temperature phosphorescent materials, *Coord. Chem. Rev.*, 2020, **404**, 213107.
25 Z. A. Yan, X. Lin, S. Sun, X. Ma and H. Tian, Activating Room-Temperature Phosphorescence of Organic Luminophores *via* External Heavy-Atom Effect and Rigidity of Ionic Polymer Matrix, *Angew. Chem., Int. Ed.*, 2021, **60**, 19735–19739.
26 Y. He, J. Wang, Q. Li, S. Qu, C. Zhou, C. Yin, H. Ma, H. Shi, Z. Meng and Z. An, Highly efficient room-temperature phosphorescence promoted *via* intramolecular-space heavy-atom effect, *Adv. Opt. Mater.*, 2023, **11**, 2201641.
27 H. Jin, X. Zhang, J. Ma, L. Bu, C. Qian, Z. Li, Y. Guan, M. Chen, Z. Ma and Z. Ma, Achieving Colorful Ultralong Organic Room-Temperature Phosphorescence by Precise Modification of Nitrogen Atoms on Phosphorescence Units, *ACS Appl. Mater. Interfaces*, 2023, **15**, 54732–54742.
28 Z. Li, Q. Yue, H. Zhang and Y. Zhao, Methodologies for constructing multi-color room temperature phosphorescent systems, *Mater. Today*, 2024, **78**, 209–230.
29 E. Hamzehpoor and D. F. Perepichka, Crystal Engineering of Room Temperature Phosphorescence in Organic Solids, *Angew. Chem., Int. Ed.*, 2019, **59**, 9977–9981.
30 H. Gao and X. Ma, Recent progress on pure organic room temperature phosphorescent polymers, *Aggregate*, 2021, **2**, e38.
31 X. Dou, X. Wang, X. Xie, J. Zhang, Y. Li and B. Tang, Advances in polymer-based organic room-temperature phosphorescence materials, *Adv. Funct. Mater.*, 2024, **34**, 2314069.
32 N. Gan, X. Zou, Z. Qian, A. Lv, L. Wang, H. Ma, H.-J. Qian, L. Gu, Z. An and W. Huang, Stretchable phosphorescent polymers by multiphase engineering, *Nat. Commun.*, 2024, **15**, 4113.
33 M. Li, X. Cai, Z. Chen, K. Liu, W. Qiu, W. Xie, L. Wang and S.-J. Su, Boosting purely organic room-temperature phosphorescence performance through a host–guest strategy, *Chem. Sci.*, 2021, **12**, 13580–13587.
34 J. Li, S. Hao, M. Li, Y. Chen, H. Li, S. Wu, S. Yang, L. Dang, S. J. Su and M. D. Li, Triplet Energy Gap-Regulated Room Temperature Phosphorescence in Host–Guest Doped Systems, *Angew. Chem., Int. Ed.*, 2024, **64**, e202417426.
35 Y. Tian, J. Yang, Z. Liu, M. Gao, X. Li, W. Che, M. Fang and Z. Li, Multistage Stimulus-Responsive Room Temperature Phosphorescence Based on Host–Guest Doping Systems, *Angew. Chem., Int. Ed.*, 2021, **60**, 20259–20263.
36 X. Jiao, W. Zhang, J. Zhi, Y. Wang, M. Wang, Z. Liu and J. Li, Ultra-long organic RTP host–guest doped systems based on pure 4-(1*H*-imidazole-1-yl)methyl benzoate as versatile hosts, *Mater. Chem. Front.*, 2025, **9**, 1166–1173.
37 Y. Zhang, S. Zhang, G. Liu, Q. Sun, S. Xue and W. Yang, Rational molecular and doping strategies to obtain organic polymers with ultralong RTP, *Chem. Sci.*, 2023, **14**, 5177–5181.
38 S. K. Mellerup and S. Wang, Boron-based stimuli responsivematerials, *Chem. Soc. Rev.*, 2019, **48**, 3537–3549.
39 H. E. Hackney and D. F. Perepichka, Recent advances in room temperature phosphorescence of crystalline boron containing organic compounds: Nanoscience: Special Issue Dedicated to Professor Paul S. Weiss, *Aggregate*, 2022, **3**, e123.
40 L. Ji, S. Griesbeck and T. B. Marder, Recent developments in and perspectives on three-coordinate boron materials: a bright future, *Chem. Sci.*, 2017, **8**, 846–863.
41 J. Dong, L. Chen and D. Yang, Rethinking boron's role in intramolecular charge transfer: from an acceptor to a donor–acceptor regulator, *Chem. Sci.*, 2025, **16**, 9577–9603.
42 Q. Liu, M. Zhang, Y. Fu, S. Shen and L. Zhu, Organoboron luminophores with extremely strong dual–phase emissions, *Chin. Chem. Lett.*, 2023, **34**, 107612.
43 H. E. Hackney and D. F. Perepichka, Recent advances in room temperature phosphorescence of crystalline boron containing organic compounds, *Aggregate*, 2021, **3**, e123.
44 H. Zheng, P. Cao, Y. Wang, X. Lu and P. Wu, Ultralong Room-Temperature Phosphorescence from Boric Acid, *Angew. Chem., Int. Ed.*, 2021, **60**, 9500–9506.
45 P. Cao, Y. Wang, H. Zheng and P. Wu, Unusual phosphorescence of boric acid: From impurity or clusterization-triggered emission?, *Aggregate*, 2024, **5**, e468.
46 Y. Song, X. Duan, Y.-N. Jiang and Y. Ma, B–O–O–B Impurity Induces Ultralong Room-Temperature Phosphorescence of Boric Acid, *J. Phys. Chem. Lett.*, 2024, **15**, 6890–6895.
47 L. Stagi, L. Malfatti, A. Zollo, S. Livraghi, D. Carboni, D. Chiriu, R. Corpino, P. C. Ricci, A. Cappai and C. M. Carbonaro, Phosphorescence by trapping defects in boric acid induced by thermal processing, *Adv. Opt. Mater.*, 2024, **12**, 2302682.

48 Z. Wu, J. C. Roldao, F. Rauch, A. Friedrich, M. Ferger, F. Würthner, J. Gierschner and T. B. Marder, Pure Boric Acid Does Not Show Room-Temperature Phosphorescence (RTP), *Angew. Chem., Int. Ed.*, 2022, **61**, e202200599.
49 Z. Li, S. Cao, Y. Zheng, L. Song, H. Zhang and Y. Zhao, Colorful ultralong room temperature phosphorescent afterglow with excitation wavelength dependence based on boric acid matrix, *Adv. Funct. Mater.*, 2024, **34**, 2306956.
50 J. Gao, X. Wu, X. Jiang, M. Li, R. He and W. Shen, Achieving purple light excitable high-efficiency temperature-responsive dual- and single-mode afterglow in carbon dots, *Carbon*, 2023, **208**, 365–373.
51 J. Deng, Z. Guan, D. Fu, Y. Zheng, Z. Chen, H. Li and X. Liu, Excitation-Dependent Long Afterglow Room-Temperature Phosphorescence Material Activated by Doping Boric Acid Matrix, *Adv. Opt. Mater.*, 2023, **11**, 2300207.
52 D. Wang, Z. Lu, X. Qin, Z. Zhang, Y. E. Shi, J. W. Lam, Z. Wang and B. Z. Tang, Boric Acid-Activated Room-Temperature Phosphorescence and Thermally Activated Delayed Fluorescence for Efficient Solid-State Photoluminescence Materials, *Adv. Opt. Mater.*, 2022, **10**, 2200629.
53 Y. Cheng, W. Fan, L. Wang, Y. Liu, S. Yang, Y. Shi, S. Liu, L. Zheng and Q. Cao, Fast photostimulus-responsive ultralong room-temperature phosphorescence behaviour of benzoic acid derivatives@ boric acid, *J. Mater. Chem. C*, 2022, **10**, 8806–8814.
54 Y. Cheng, W. Fan, R. He, X. Meng, Q. Zhou, X. Ma, Y. Liu, Y. Shi, L. Zheng and Q. Cao, Naphthoic Acid Derivatives@ Boric Acid Based Fast Photo-Activated Room-Temperature Phosphorescence Materials with Dynamic Changed Emission Color, *Adv. Opt. Mater.*, 2024, **12**, 2303017.
55 Z. Li, S. Cao, Y. Zheng, L. Song, H. Zhang and Y. Zhao, Colorful Ultralong Room Temperature Phosphorescent Afterglow with Excitation Wavelength Dependence Based on Boric Acid Matrix, *Adv. Funct. Mater.*, 2023, **34**, 2306956.
56 L. Guan, Q. Huang, R. Yang, S. Jiang, Y. Zhuang, P. Wang, Y. Gao, R. J. Xie, Q. Ling and Z. Lin, Hour-Level and Air-Stable Organic Long-Persistent Luminescence from Organic–Inorganic Hybrid Materials, *Adv. Mater.*, 2025, **37**, 2419213.
57 R. Kabe and C. Adachi, Organic long persistent luminescence, *Nature*, 2017, **550**, 384–387.
58 S. Kuno, T. Kanamori, Z. Yijing, H. Ohtani and H. Yuasa, Long persistent phosphorescence of crystalline phenylboronic acid derivatives: photophysics and a mechanistic study, *ChemPhotoChem*, 2017, **1**, 102–106.
59 Z. Chai, C. Wang, J. Wang, F. Liu, Y. Xie, Y.-Z. Zhang, J.-R. Li, Q. Li and Z. Li, Abnormal room temperature phosphorescence of purely organic boron-containing compounds: the relationship between the emissive behaviorand the molecular packing, and the potential related applications, *Chem. Sci.*, 2017, **8**, 8336–8344.
60 M. Liu, Z. Mao, Y. Wang, W. Kong, J. Huang, W. Li, Z. Yang, X. Huang, W. S. Zou and H. Q. Yu, Activating Ultralong Room-Temperature Phosphorescence of Mono-Ring Arylboronic Acid by Hydrogen Bond for Tunable Afterglow Color and Stimulus Response, *Small*, 2025, **21**, 2407079.
61 J. Zhang, S. Xu, Z. Wang, P. Xue, W. Wang, L. Zhang, Y. Shi, W. Huang and R. Chen, Stimuli-responsive deep-blue organic ultralong phosphorescence with lifetime over 5 s for reversible water-jet anti-counterfeiting printing, *Angew. Chem., Int. Ed.*, 2021, **60**, 17094–17101.
62 W.-G. Chen, Y.-F. Zhuang, Y. Wang, Z.-J. Chen, Y.-F. Lv, F. Song and Y. Chen, Visible-light excitable polymers with ultra-long phosphorescence afterglow achieved by boron-based dative bonds, *Chem. Eng. J.*, 2025, **503**, 158381.
63 Z. He, J. Song, C. Li, Z. Huang, W. Liu and X. Ma, High-Performance Organic Ultralong Room Temperature Phosphorescence Based on Biomass Macrocycle, *Adv. Mater.*, 2025, **37**, 2418506.
64 Y. Xie, Z. Wang, M. Zhang, X. Wu, Y. Sun, J. Wu, C.-L. Sun, B. Zhang and X. Pan, Cluster-triggered excitation-dependent phosphorescence emission in polymorphic arylborinic acid, *Inorg. Chem. Commun.*, 2024, **168**, 112895.
65 Y. Shoji, Y. Ikabata, Q. Wang, D. Nemoto, A. Sakamoto, N. Tanaka, J. Seino, H. Nakai and T. Fukushima, Unveiling a new aspect of simple arylboronic esters: long-lived room-temperature phosphorescence from heavy-atom-free molecules, *J. Am. Chem. Soc.*, 2017, **139**, 2728–2733.
66 Z. Wu, C. Herok, A. Friedrich, B. Engels, T. B. Marder and Z. M. Hudson, Impurities in arylboronic esters induce persistent afterglow, *J. Am. Chem. Soc.*, 2024, **146**, 31507–31517.
67 K. Zhang, Q. Sun, L. Tang, Y. Wang, X. Fan, L. Liu, S. Xue and W. Yang, Cyclic boron esterification: screening organic room temperature phosphorescent and mechanoluminescent materials, *J. Mater. Chem. C*, 2018, **6**, 8733–8737.
68 H. Sun, Z. Xie, H. Wang, Y. Wu, B. Du, C. Guan and T. Yu, Manipulating room-temperature phosphorescence *via* lone-pair electrons and empty-orbital arrangements and hydrogen bond adjustment, *J. Mater. Chem. C*, 2022, **10**, 8854–8859.
69 Z. Wu, J. Nitsch, J. Schuster, A. Friedrich, K. Edkins, M. Loebnitz, F. Dinkelbach, V. Stepanenko, F. Würthner and C. M. Marian, Persistent room temperature phosphorescence from triarylboranes: a combined experimental and theoretical study, *Angew. Chem., Int. Ed.*, 2020, **59**, 17137–17144.
70 J. Jovaišaitė, S. Kirschner, S. Raišys, G. Kreiza, P. Baronas, S. Juršėnas and M. Wagner, Diboraanthracene-Doped Polymer Systems for Colour-Tuneable Room-Temperature Organic Afterglow, *Angew. Chem., Int. Ed.*, 2023, **62**, e202215071.
71 Z. Wu, F. Dinkelbach, F. Kerner, A. Friedrich, L. Ji, V. Stepanenko, F. Würthner, C. M. Marian and T. B. Marder, Aggregation-Induced Dual Phosphorescence from (*o*-Bromophenyl)-Bis (2, 6-Dimethylphenyl) Borane at Room Temperature, *Chem. – Eur. J.*, 2022, **28**, e202200525.
72 J.-L. Ma, H. Liu, S.-Y. Li, Z.-Y. Li, H.-Y. Zhang, Y. Wang and C.-H. Zhao, Metal-free room-temperature phosphorescence from amorphous triarylborane-based biphenyl, *Organometallics*, 2020, **39**, 4153–4158.
73 H. Ding, Y. Sun, M. Tang, J. Wen, S. Yue, Y. Peng, F. Li, L. Zheng, S. Wang and Y. Shi, Time-dependent photo-

activated aminoborane room-temperature phosphorescence materials with unprecedented properties: simple, versatile, multicolor-tuneable, water resistance, optical information writing/erasing, and multilevel data encryption, *Chem. Sci.*, 2023, **14**, 4633–4640.

74 X. Cai, Y. Sun, W. He, Y. Zheng, Y. Shi and Q. Cao, Multifunctional Amino-Boranes Isomer Room-Temperature Phosphorescent Material: Multi-Substrate Multicolor Luminescence, Multi-Level Anti-Counterfeiting, Light-Controlled Data Erasing/Writing, Data Logic Operation, and High Anti-Laundry Detergent Performance, *Adv. Funct. Mater.*, 2024, **34**, 2407420.

75 R. Arumugam, A. T. M. Munthasir, R. Kannan, D. Banerjee, P. Sudhakar, V. R. Soma, P. Thilagar and V. Chandrasekhar, Regioisomers containing triarylboron-based motifs as multifunctional photoluminescent materials: from dual-mode delayed emission to pH-switchable room-temperature phosphorescence, *Chem. Sci.*, 2024, **15**, 18364–18378.

76 Y. Shi, Y. Zeng, P. Kucheryavy, X. Yin, K. Zhang, G. Meng, J. Chen, Q. Zhu, N. Wang, X. Zheng, F. Jäkle and P. Chen, Dynamic B/N Lewis Pairs: Insights into the Structural Variations and Photochromism *via* Light-Induced Fluorescence to Phosphorescence Switching, *Angew. Chem., Int. Ed.*, 2022, **61**, e202213615.

77 L. Tu, Y. Fan, C. Bi, L. Xiao, Y. Li, A. Li, W. Che, Y. Xie, Y. Zhang, S. Xu, W. Xu, Q. Li and Z. Li, How temperature and hydrostatic pressure impact organic room temperature phosphorescence from H-aggregation of planar triarylboranes and the application in bioimaging, *Sci. China: Chem.*, 2023, **66**, 816–825.

78 L. Tu, Y. Chen, X. Song, W. Jiang, Y. Xie and Z. Li, Förster resonance energy transfer: stimulus-responsive purely organic room temperature phosphorescence through dynamic B–N bond, *Angew. Chem., Int. Ed.*, 2024, **63**, e202402865.

79 A. N. Bismillah and I. Aprahamian, Boron difluoride hydrazone (BODIHY) complexes: A new class of fluorescent molecular rotors, *J. Phys. Org. Chem.*, 2023, **36**, e4485.

80 Q. Qi, S. Huang, X. Liu and I. Aprahamian, 1, 2-BF2 Shift and photoisomerization induced multichromatic response, *J. Am. Chem. Soc.*, 2024, **146**, 6471–6475.

81 N. D. Nguyen, G. Zhang, J. Lu, A. E. Sherman and C. L. Fraser, Alkyl chain length effects on solid-state difluoroboron β-diketonate mechanochromic luminescence, *J. Mater. Chem.*, 2011, **21**, 8409–8415.

82 D. Cappello, A. E. Watson and J. B. Gilroy, A Boron Difluoride Hydrazone (BODIHY) Polymer Exhibits Aggregation-Induced Emission, *Macromol. Rapid Commun.*, 2021, **42**, 2000553.

83 P.-Z. Chen, L.-Y. Niu, Y.-Z. Chen and Q.-Z. Yang, Difluoroboron β-diketonate dyes: Spectroscopic properties and applications, *Coord. Chem. Rev.*, 2017, **350**, 196–216.

84 G. Zhang, J. Lu, M. Sabat and C. L. Fraser, Polymorphism and reversible mechanochromic luminescence for solid-state difluoroboron avobenzone, *J. Am. Chem. Soc.*, 2010, **132**, 2160–2162.

85 B. Xu, G. Wang, H. Gao, T. Wang, Z. Ye, W. Xia, Q. Chong, Q. Yan and K. Zhang, Bright organic long persistent luminescence in difluoroboron β-Diketonate systems, *Chem. Eng. J.*, 2025, **514**, 163359.

86 X. Sun, X. Zhang, X. Li, S. Liu and G. Zhang, A mechanistic investigation of mechanochromic luminescent organoboron materials, *J. Mater. Chem.*, 2012, **22**, 17332–17339.

87 X. Chen, G. Wang, J. Li, X. Chen, X. Zhao, Y. Zeng, Y. Su and K. Zhang, Difluoroboron β-diketonate systems: large transformation of photophysical mechanism induced by tiny structural modification or isomerization, *Adv. Opt. Mater.*, 2024, **12**, 2301619.

88 G. Zhang, G. M. Palmer, M. W. Dewhirst and C. L. Fraser, A dual-emissive-materials design concept enables tumour hypoxia imaging, *Nat. Mater.*, 2009, **8**, 747–751.

89 A. Pfister, G. Zhang, J. Zareno, A. F. Horwitz and C. L. Fraser, Boron polylactide nanoparticles exhibiting fluorescence and phosphorescence in aqueous medium, *ACS Nano*, 2008, **2**, 1252–1258.

90 G. Wang, X. Chen, J. Liu, S. Ding and K. Zhang, Advanced charge transfer technology for highly efficient and long-lived TADF-type organic afterglow with near-infrared light-excitable property, *Sci. China: Chem.*, 2023, **66**, 1120–1131.

91 X. Chen, G. Wang, X. Piao and K. Zhang, Achieving Visible-Light-Excitable Blue TADF-Type Afterglow *via* Delicate Control of Excited States in Difluoroboron β-Diketonate Systems, *Chem. – Eur. J.*, 2024, **30**, e202303834.

92 G. Zhang, J. Chen, S. J. Payne, S. E. Kooi, J. Demas and C. L. Fraser, Multi-emissive difluoroboron dibenzoylmethane polylactide exhibiting intense fluorescence and oxygen-sensitive room-temperature phosphorescence, *J. Am. Chem. Soc.*, 2007, **129**, 8942–8943.

93 J. Xiang, H. Qin, J. Zou, J. Jiang, P. Geng, J. Yan and S. Xiao, Polymorphic β-diketone boron-difluoride crystals with distinct room temperature phosphorescence aroused by tiny differences in intermolecular interactions, *Dyes Pigm.*, 2023, **216**, 111378.

94 L. Qiu, Z. Chen, J. Wu, G. Zeng, X. Liu, K. Liu, S.-J. Su, J. Loos and T. Wen, Room-temperature phosphorescence induced by heterogeneous polymer matrixes, *Macromolecules*, 2024, **57**, 2679–2686.

95 A. Sakai, E. Ohta, Y. Matsui, S. Tsuzuki and H. Ikeda, Room-Temperature Phosphorescence of Crystalline Metal-Free Organoboron Complex, *ChemPhysChem*, 2016, **17**, 4033–4036.

96 T. Liu, G. Zhang, R. E. Evans, C. O. Trindle, Z. Altun, C. A. DeRosa, F. Wang, M. Zhuang and C. L. Fraser, Phosphorescence tuning through heavy atom placement in unsymmetrical difluoroboron β-diketonate materials, *Chem. – Eur. J.*, 2018, **24**, 1859–1869.

97 C. A. DeRosa, M. L. Daly, C. Kerr and C. L. Fraser, Methoxy-Substituted Difluoroboron Benzoylacetonate Complexes with Color-Tunable Phosphorescence, *ChemPhotoChem*, 2019, **3**, 31–36.

98 J. Li, X. Li, G. Wang, X. Wang, M. Wu, J. Liu and K. Zhang, A direct observation of up-converted room-temperature phosphorescence in an anti-Kasha dopant-matrix system, *Nat. Commun.*, 2023, **14**, 1987.

99 X. Piao, X. Li, G. Wang, T. Wang and K. Zhang, Room-temperature phosphorescence of natural silkworm cocoon silk, *ACS Mater. Lett.*, 2024, **6**, 2231–2238.
100 X. Piao, T. Wang, X. Chen, G. Wang, X. Zhai and K. Zhang, Room-temperature phosphorescent transparent wood, *Nat. Commun.*, 2025, **16**, 868.
101 G. Wang, X. Chen, Y. Zeng, X. Li, X. Wang and K. Zhang, Dual-Mechanism Design Strategy for High-Efficiency and Long-Lived Organic Afterglow Materials, *J. Am. Chem. Soc.*, 2024, **146**, 24871–24883.
102 Q. Chong, B. Xu, G. Wu, H. Gao, Y. Zhang, Q. Yan, B. Wang and K. Zhang, Thermally Activated Delayed Fluorescence-Type Organic Afterglow Emitters for Devising Organic Long Persistent Luminescence Materials, *ACS Mater. Lett.*, 2025, **7**, 1313–1320.
103 J. Li, X. Wang, Y. Pan, Y. Sun, G. Wang and K. Zhang, Unexpected long room-temperature phosphorescence lifetimes of up to 1.0 s observed in iodinated molecular systems, *Chem. Commun.*, 2021, **57**, 8794–8797.
104 S.-S. Gong, X.-Z. Tan, R.-X. Yang, C.-H. Cao, C. Zheng, Y.-X. Li, H. Zheng, G. Li, S. Pu, R. Shi, Z. Chen and Q. Sun, Converting aggregation-induced emission of N-BF2 merocyanines to colour-tunable ultralong room temperature phosphorescence *via* Dexter triplet energy transfer: circumventing restriction of intersystem crossing, *J. Mater. Chem. C*, 2025, **13**, 8265–8273.
105 P. Samadder, K. Naim, S. C. Sahoo and P. P. Neelakandan, Surface coating induced room-temperature phosphorescence in flexible organic single crystals, *Chem. Sci.*, 2024, **15**, 9258–9265.
106 S. Li, L. Fu, X. Xiao, H. Geng, Q. Liao, Y. Liao and H. Fu, Regulation of Thermally Activated Delayed Fluorescence to Room-Temperature Phosphorescent Emission Channels by Controlling the Excited-States Dynamics *via* J- and H-Aggregation, *Angew. Chem., Int. Ed.*, 2021, **60**, 18059–18064.
107 M. Koch, K. Perumal, O. Blacque, J. A. Garg, R. Saiganesh, S. Kabilan, K. K. Balasubramanian and K. Venkatesan, Metal-Free Triplet Phosphors with High Emission Efficiency and High Tunability, *Angew. Chem., Int. Ed.*, 2014, **53**, 6378–6382.
108 Z. Yu, Y. Wu, L. Xiao, J. Chen, Q. Liao, J. Yao and H. Fu, Organic Phosphorescence Nanowire Lasers, *J. Am. Chem. Soc.*, 2017, **139**, 6376–6381.
109 A. Lv, W. Ye, X. Jiang, N. Gan, H. Shi, W. Yao, H. Ma, Z. An and W. Huang, Room-temperature phosphorescence from metal-free organic materials in solution: Origin and molecular design, *J. Phys. Chem. Lett.*, 2019, **10**, 1037–1042.
110 L. Xiao, Y. Wu, Z. Yu, Z. Xu, J. Li, Y. Liu, J. Yao and H. Fu, Room-Temperature Phosphorescence in Pure Organic Materials: Halogen Bonding Switching Effects, *Chem. – Eur. J.*, 2018, **24**, 1801–1805.
111 W. Wang, S. Tong, Q. Q. Wang, Y. F. Ao, D. X. Wang and J. Zhu, Thiazole Boron Difluoride Dyes with Large Stokes Shift, Solid State Emission and Room-Temperature Phosphorescence, *Chem. – Eur. J.*, 2022, **28**, e202202507.
112 X. Wang, X. Wu, T. Wang, Y. Wu, H. Shu, Z. Cheng, L. Zhao, H. Tian, H. Tong and L. Wang, A high-contrast polymorphic difluoroboron luminogen with efficient RTP and TADF emissions, *Chem. Commun.*, 2023, **59**, 1377–1380.
113 A. E. R. Watson, S. Y. Tao, A. Siemiarczuk, P. D. Boyle, P. J. Ragogna and J. B. Gilroy, Organic Room Temperature Phosphorescence from BN-Substituted Xanthene Derivatives, *Angew. Chem., Int. Ed.*, 2024, **64**, e202414534.